bioRxiv preprint doi: https://doi.org/10.1101/308080; this version posted May 26, 2018. The copyright holder for this preprint (which was not certified by peer review) is the author/funder. All rights reserved. No reuse allowed without permission.

Identification of a novel subfamily of bacterial AAT-fold basic amino acid decarboxylases and functional characterization of its first representative: *Pseudomonas aeruginosa* LdcA

Diego Carriel-Lopez,[1,2,#] Pierre Simon Garcia,[3,4,#] Florence Castelli,[5] Patricia Lamourette,[5] François Fenaille,[5] Céline Brochier-Armanet,[3,4,*] Sylvie Elsen[2,] and Irina Gutsche[1,***]**

[1]University of Grenoble Alpes, CNRS, CEA, CNRS, IBS, F-38000 Grenoble, France

[2]Biology of Cancer and Infection, U1036 INSERM, CEA, University of Grenoble Alpes, ERL5261 CNRS, Grenoble, France

[3]Université Lyon 1, CNRS, UMR5558, Laboratoire de Biométrie et Biologie Évolutive, F-69622, Villeurbanne, France

[4]MMSB Molecular Microbiology and Structural Biochemistry, Institut de Biologie et de Chimie des Protéines 69367 LYON cedex 07, France

[5]Service de Pharmacologie et Immuno-Analyse (SPI), Laboratoire d'Etude du Métabolisme des Médicaments, CEA, INRA, Université Paris Saclay, MetaboHUB, F-91191 Gif-sur-Yvette, France

For correspondence. *E-mail celine.brochier-armanet@univ-lyon1.fr; Tel. (33) 426234476; Fax (33) 472431388; **E-mail sylvie.elsen@cea.fr; Tel. (33) 438783074; Fax (33) 438785058; ***E-mail irina.gutsche@ibs.fr; Tel. (33) 457428766; Fax (33) 438785122.

Short Title: LdcA, a new phylogenetic family of bacterial Ldcs

Key words: bacterial amino acid decarboxylases, polyamines, evolution, lysine decarboxylase, *Pseudomonas aeruginosa*

[#]These authors contributed equally to this work

bioRxiv preprint doi: https://doi.org/10.1101/308080; this version posted May 26, 2018. The copyright holder for this preprint (which was not certified by peer review) is the author/funder. All rights reserved. No reuse allowed without permission.

Summary

Polyamines are small amino-acid derived polycations capable of binding negatively charged macromolecules. Bacterial polyamines are structurally and functionally diverse, and are mainly produced biosynthetically by PLP-dependent amino acid decarboxylases referred to as LAOdcs (Lysine-Arginine-Ornithine decarboxylases). In a phylogenetically limited group of bacteria, LAOdcs are also induced in response to acid stress. Here, we performed an exhaustive phylogenetic analysis of the AAT-fold LAOdcs which showcased the ancestral nature of their short forms in *Cyanobacteria* and *Firmicutes*, and emergence of distinct subfamilies of long LAOdcs in *Proteobacteria*. We identified a novel subfamily of lysine decarboxylases, LdcA, ancestral in *Betaproteobacteria* and *Pseudomonadaceae* (*Gammaproteobacteria*). We analyzed the expression of LdcA from *Pseudomonas aeruginosa*, and uncovered its role, intimately linked to cadaverine production, in promoting growth and reducing persistence of this multidrug resistant human pathogen during carbenicillin treatment. Finally, we documented a certain redundancy in the function of the three main polyamines - cadaverine, putrescine and spermidine – in *P. aeruginosa* by demonstrating the link between their intracellular level, as well as the capacity of putrescine and spermidine to complement the growth phenotype of the *ldcA* mutant.

Introduction

Polyamines are small amino acid-derived molecules with two or more amino groups separated by alkyl chains (Tabor & Tabor, 1964, Lightfoot & Hall, 2014). They perform essential functions in all living organisms by participating in DNA replication, gene expression and protein synthesis, and are generally described as growth factors (Lightfoot & Hall, 2014, Michael, 2016b). At physiological pH, polyamines behave as polycations and can interact with negatively charged macromolecules such as nucleic acids, membrane phospholipids and proteins (Tabor & Tabor,

bioRxiv preprint doi: https://doi.org/10.1101/308080; this version posted May 26, 2018. The copyright holder for this preprint (which was not certified by peer review) is the author/funder. All rights reserved. No reuse allowed without permission.

1964, Tabor & Tabor, 1985). They were proposed to bind and structurally modify RNA thereby acting at the level of translation (Igarashi & Kashiwagi, 2006, Igarashi & Kashiwagi, 2015). Strengthening this hypothesis, "polyamine modulons" were identified in *Escherichia coli* and more recently in eukaryotes (Igarashi & Kashiwagi, 2006, Igarashi & Kashiwagi, 2015). As a possible consequence, bacterial polyamines were shown to participate in expression of proteins essential for growth fitness and viability but also in processes such as biofilm formation, antibiotic resistance and virulence (Kwon & Lu, 2006, Shah & Swiatlo, 2008, Karatan & Michael, 2013, Di Martino *et al.*, 2013, Michael, 2016a) .

The triamine spermidine (Spd), essential in eukaryotes and archaea (Lightfoot & Hall, 2014, Michael, 2016b), and its diamine precursor putrescine (Put) are extensively studied because these two polyamines are the only ones produced in all eukaryotes (Michael, 2016b). In bacteria, the polyamine repertoire and hence their roles are the most diverse. In particular, a third widespread bacterial polyamine, cadaverine (Cad), appears increasingly important for the physiology of *Proteobacteria*. Cad is recognized as an important player in enterobacterial acid stress response wherein it decreases porin permeability to protons and alkalinizes the medium (Dela Vega & Delcour, 1996, Zhao & Houry, 2010). During oxidative stress response, Cad is also capable of scavenging reactive oxygen species (ROS) in *Vibrio vulnificus* (Kang *et al.*, 2007). In some Negativicutes, *Selenomonas ruminantium* and *Veillonella sp.,* Cad was shown to be incorporated in the peptidoglycan and essential for its stability (Kamio *et al.*, 1986, Kamio & Nakamura, 1987). Finally, this polyamine is involved in iron uptake and is required for the synthesis of hydroxamate-type siderophores in different bacterial species such as *Streptomyces coelicolor* (Burrell *et al.*, 2012).

bioRxiv preprint doi: https://doi.org/10.1101/308080; this version posted May 26, 2018. The copyright holder for this preprint (which was not certified by peer review) is the author/funder. All rights reserved. No reuse allowed without permission.

Polyamine biosynthesis depends on the activity of basic amino acid decarboxylases using Lysine, Arginine or Ornithine as specific substrate to produce Cad, Agmatine (Agm) or Put, respectively. These enzymes can therefore be generally referred to as LAOdcs (Lysine-Arginine-Ornithine decarboxylases). In most eukaryotes, Put synthesis is carried out by an ornithine decarboxylase (Odc) (Michael, 2016a, Michael, 2016b). An alternative pathway for Put biosynthesis found in bacteria and plants involves decarboxylation of arginine by arginine decarboxylases (Adc); these enzymes produce Agm which is further converted into Put by agmatine iminohydrolase/deiminase and N-carbamoylputrescine amidohydrolase (Michael, 2016a, Michael, 2016b). Interestingly, plants (Lee & Cho, 2001, Bunsupa *et al.*, 2012) and some bacteria exemplified by *S. ruminantium* and *V. vulnificus* (Takatsuka *et al.*, 2000, Lee *et al.*, 2007) possess a bifunctional Odc/Ldc capable of synthesizing both Put and Cad. Spd is formed by spermidine synthase (SpdSyn) through aminopropylation of Put, using an aminopropyl group released by decarboxylation of S-adenosylmethionine (Michael, 2016a, Michael, 2016b). In addition, *E. coli* SpdSyn transforms Cad into aminopropyl-Cad, a Spd analogue sharing its growth stimulating properties (Kim *et al.*, 2016).

Two major structural protein super-families are responsible for polyamine biosynthesis through pyridoxal-5-phosphate (PLP)-dependent LAOdcs: the alanine racemase fold (AR-fold) super-family and the aspartate aminotransferase fold (AAT-fold) super-family (Eliot & Kirsch, 2004). Phylogenetic studies of the LAOdcs of the AR-fold super-family revealed that these enzymes are widespread throughout the three domains of life while the AAT-fold LAOdcs are found exclusively in Bacteria and a few archaea (Lee *et al.*, 2007, Burrell *et al.*, 2010). Bacterial AAT-fold LAOdcs can be divided in two types according to the presence or absence of a

bioRxiv preprint doi: https://doi.org/10.1101/308080; this version posted May 26, 2018. The copyright holder for this preprint (which was not certified by peer review) is the author/funder. All rights reserved. No reuse allowed without permission.

95 particular CheY-like response regulator receiver domain, known as the "wing domain",
96 necessary for the formation of higher-order oligomers (Burrell *et al.*, 2010, Kanjee *et al.*, 2011b).
97 The short form referred as wing-less LAOdc was found in *Firmicutes*, *Cyanobacteria* and
98 *Actinobacteria* phyla, and a few "wing-less" AAT-fold decarboxylases from *Firmicutes* and
99 *Actinobacteria* were shown to have an Adc activity, required in particular for biofilm formation
100 in *Bacillus subtilis* (*Firmicutes*) (Burrell *et al.*, 2010). The long, wing domain-containing form
101 likely originated in *Proteobacteria* (Kanjee *et al.*, 2011b).

102 AAT-fold decarboxylases with the wing domain have been intensively studied in
103 *Enterobacteria* since the early 1940s (Gale & Van Heyningen, 1942, Gale & Epps, 1944) because
104 of the link between enterobacterial pathogenicity for humans and their capacity to withstand
105 acid stress thanks to the crucial role of the inducible LAOdcs. Consequently, the current
106 understanding of the AAT-fold LAOdc is based on analyses of a very limited number of bacterial
107 species, *i.e.* mostly *enterobacteria: E. coli*, *Salmonella typhimurium*, *Vibrio cholerae* and *V.*
108 *vulnificus*. At a specific acidic pH, expression of the decarboxylase gene is induced by an excess
109 of the target amino acid uptaken by a dedicated inner membrane antiporter (Kanjee & Houry,
110 2013). The enzyme transforms the amino acid substrate into the corresponding polyamine upon
111 consumption of a proton and production of a CO_2 molecule. In association with the polyamine
112 excretion by the antiporter, this reaction results in an efficient buffering of the intracellular
113 medium and the extracellular surroundings. These inducible stress response decarboxylases are
114 distinguished from "biosynthetic" enzymes that are involved only in polyamine biosynthesis. *E.*
115 *coli* encodes two biosynthetic decarboxylases (LdcC: Lys->Cad and OdcC/SpeC: Orn->Put)
116 responsible for Cad and Put biosynthesis respectively, and three acid stress-inducible

bioRxiv preprint doi: https://doi.org/10.1101/308080; this version posted May 26, 2018. The copyright holder for this preprint (which was not certified by peer review) is the author/funder. All rights reserved. No reuse allowed without permission.

decarboxylases (LdcI: Lys->Cad, AdcI/AdiA: Arg->Agm and OdcI/SpeF: Orn->Put) which together constitute a very robust acid stress response system that allows the bacterium to survive upon acid stress as low as pH 2.0 (Zhao & Houry, 2010, Kanjee *et al.*, 2011a, Kanjee & Houry, 2013). The importance of LdcI was also demonstrated in *S. typhimurium, V. cholerae* and *V. vulnificus*, where it promotes growth and survival under acidic conditions but also confers protection from oxidative stress insults (Merrell & Camilli, 2000, Kang *et al.*, 2007, Viala *et al.*, 2011)). It should be noted that LdcI-encoding genes are often designated as *cadA* as originally proposed upon identification of this gene in *E. coli* (Tabor *et al.*, 1980).

E. coli LdcI but not LdcC interacts with the AAA+ ATPase RavA to assemble into a huge macromolecular cage (Snider *et al.*, 2006, El Bakkouri *et al.*, 2010, Malet *et al.*, 2014, Kandiah *et al.*, 2016). One of the functions of this mysterious complex is to protect LdcI from inhibition by the stringent response alarmone ppGpp, thus enabling the bacterium to efficiently cope with both acid and nutrient stress simultaneously (El Bakkouri *et al.*, 2010, Kanjee *et al.*, 2011a, Malet *et al.*, 2014). While investigating why RavA binds only LdcI but not LdcC, we documented numerous inconsistencies in annotation of enterobacterial *ldcI* and *ldcC* genes and realized that each of these two families appeared to have a distinct genetic context (Kandiah *et al.*, 2016). Thus, spurred on by the limited nature of the previous studies, we set out to perform an extensive phylogenetic analysis of the AAT-fold LAOdcs in circa 4,500 complete prokaryotic proteomes to decipher the evolutionary history of these proteins and their functional evolution. In the present study, we revealed the ancestral nature of the wing-less LAOdcs in *Cyanobacteria* and *Firmicutes*, and the complex evolutionary history of long AAT-fold LAOdcs in *Proteobacteria*, leading to the emergence of distinct subfamilies. Moreover, we disclosed a novel subfamily of

bioRxiv preprint doi: https://doi.org/10.1101/308080; this version posted May 26, 2018. The copyright holder for this preprint (which was not certified by peer review) is the author/funder. All rights reserved. No reuse allowed without permission.

enzymes, clearly distinct from the well-known LdcI, LdcC, AdcI, OdcI and OdcC families, but more related to Ldc and Adc than to Odc. Excitingly, this novel evolutionary subfamily has been overlooked in previous phylogenetic analyses in spite of its wide distribution in *Betaproteobacteria* and *Pseudomonadaceae*, implying that it deserves a thorough characterization and a functional comparison with the known AAT-fold long LAOdc. The only previously mentioned LAOdc from these taxa is the lysine decarboxylase LdcA from a major multidrug resistant opportunistic human pathogen *Pseudomonas aeruginosa* (Chou *et al.*, 2010). Thus, here we went beyond the initial characterization of the *P. aeruginosa* LdcA (Chou *et al.*, 2010), and further analyzed its expression, regulation, and function in the light of the available knowledge in particular on *E. coli* LdcI and LdcC. This combined phylogenetic and functional study revealed that LdcA belongs to a novel subgroup of the long AAT-fold LAOdcs, and that its function is linked to Cad production and to the general polyamine metabolism rather than to stress response.

Results

Taxonomic distribution of AAT-fold LAOdcs in prokaryotes

An in-depth survey of 4,466 prokaryotic proteomes representing 1,904 species revealed 4,090 protein sequences belonging to the AAT-fold LAOdcs (13 of which were unannotated or annotated as pseudo-genes) (Fig. S1A). Representatives of this super-family are mainly present in Bacteria, especially in *Proteobacteria*, *Firmicutes*, *Actinobacteria* and *Cyanobacteria*, while only seven sequences were detected in *Archaea* (Fig. S1A), indicating that AAT-fold LAOdc are very likely of bacterial origin. The corresponding Maximum Likelihood (ML) tree could be

bioRxiv preprint doi: https://doi.org/10.1101/308080; this version posted May 26, 2018. The copyright holder for this preprint (which was not certified by peer review) is the author/funder. All rights reserved. No reuse allowed without permission.

divided in three parts (Fig. S1B). Cluster I encompasses sequences devoid of the wing domain (short AAT-fold LAOdc) (Bootstrap value (BV) = 99%). They are mainly found in *Firmicutes*, *Cyanobacteria* and *Actinobacteria*. Cluster II gathers nearly all proteobacterial sequences and a few sequences from *Firmicutes* (BV = 99%), all containing a wing domain. Cluster III branches in-between Cluster I and Cluster II; it is composed of a mix of long and short AAT-fold LAOdc sequences from unrelated taxonomic groups (*Proteobacteria*, *Actinobacteria*, *Bacteroidetes*, and *Firmicutes*), strongly suggesting that they spread through horizontal gene transfers among these lineages.

Wingless AAT-fold LAOdc are ancestral in Firmicutes and Cyanobacteria

Within Cluster I, all cyanobacterial sequences group together albeit with a weak bootstrap value (BV) (Fig. 1A). They are widely distributed in this phylum (Fig. 2). The phylogeny inferred with these sequences (Fig. 2A) is overall consistent with a reference phylogeny of *Cyanobacteria* based on ribosomal proteins (Fig. 2B). This indicates that a gene coding for a wing-less AAT-fold LAOdc was likely present in the ancestor of *Cyanobacteria* and had been mainly transmitted vertically in *Cyanobacteria*. The genomic context of LAOdc in *Cyanobacteria* is not conserved even in relatively close species (Fig. 2C).

Similarly, sequences of *Firmicutes* belonging to Cluster I are widely distributed in this phylum (Fig. 1). The comparison of the phylogeny inferred with these sequences (Fig. 1A) with a reference phylogeny of *Firmicutes* (Fig. 1B) suggests that a gene coding for a short AAT-fold LAOdc was present in the ancestor of this phylum. Noteworthy, most of members of *Firmicutes* harbor two LAOdc copies (referred as A and B), with exception of the most early-branching

bioRxiv preprint doi: https://doi.org/10.1101/308080; this version posted May 26, 2018. The copyright holder for this preprint (which was not certified by peer review) is the author/funder. All rights reserved. No reuse allowed without permission.

lineages: one single gene corresponding to the copy A is found in *Natranaerobiaceae*, while no gene is found in *Halobacteroidaceae* and *Halanaerobiaceae* (Fig. 1B). These two copies can be easily distinguished by their genomic context (Fig. 1C): the copy A presents a well-conserved association with thymidylate kinase and DNA polymerase III subunit delta coding genes, while the genomic context of copy B was not conserved. The presence of gene coding for a copy A in the early diverging *Natranaerobiaceae* lineage and in most *Firmicutes* taxa suggests that the copy A could be ancestral in *Firmicutes*. In contrast, the copy B seems to appear in the common ancestor shared by *Clostridia* and *Bacilli,* possibly as the result of a gene duplication event. Worthy of note, a loss of both copies can be inferred in the ancestor of *Lactobacillales*. Yet, some *Streptococcaceae* and *Carnobacteriaceae* have reacquired either copy A or copy B by horizontal gene transfer from different *Firmicutes* donors (Fig. 1A). Finally, Cluster I encompassed a group of sequences from *Actinobacteria*. Their taxonomic distribution is patchy and their phylogeny is not consistent with the current taxonomy, suggesting that they have been acquired and spread through horizontal gene transfer in *Actinobacteria*.

Wing-domain containing AAT-fold LAOdc form four groups in Proteobacteria

The phylogenetic analysis of proteobacterial AAT-fold LAOdcs composing the Cluster II revealed two monophyletic groups, corresponding to Odc (Posterior probabilities (PP) = 1, Fig. 3A and BV = 100%, Fig. 3B) and LAdc (PP = 1, Fig. 3A and BV = 100%, Fig. 3B). The LAdc group is further split into LdcI/LdcC (PP = 1, Fig. 3A and BV = 100%, Fig. 3B), Adc (PP = 1, Fig. 3A and BV = 93, Fig. 3B), and a hitherto non-identified subfamily (PP = 1, Fig. 3A and BV =100%, Fig. 3B), that will be referred as LdcA in the name of its only previously mentioned member, LdcA from *P.*

bioRxiv preprint doi: https://doi.org/10.1101/308080; this version posted May 26, 2018. The copyright holder for this preprint (which was not certified by peer review) is the author/funder. All rights reserved. No reuse allowed without permission.

205 *aeruginosa* (Chou *et al.*, 2010). It should be emphasized that although the monophyly of
206 OdcI/OdcC, LdcI/LdcC, Adc and LdcA groups is well supported, the relationships among
207 LdcI/LdcC, Adc and LdcA are unresolved (PP = 0.67, Fig. 3A and BV < 80%, Fig. 3B).

208 The comparison of the LAOdc phylogeny (Fig. 3B) and taxonomic distribution with a
209 reference phylogeny of *Proteobacteria* (Fig. 4A) suggests that *odcI* could be ancestral in
210 *Bradyrhizobiaceae*, *Xanthobacteriaceae*, *Methylobacteriaceae*, and *Beijerinckiaceae* (all
211 belonging to *Alphaproteobacteria*), as well as in *Vibrionaceae*, *Pasteurellaceae*, and
212 *Enterobacteriaceae* (all belonging to *Gammaproteobacteria*). In contrast, *odcC* seems more
213 recent and appears to result from a gene duplication of *odcI* that occurred in
214 *Enterobacteriaceae*, before the divergence of *Sodalis* (PP = 1, Fig. 3A and BV = 75%, Fig. 3B, and
215 Fig. 4B). Genes coding for OdcI and OdcC are clearly distinguished by their context (Fig. S2).
216 More precisely, *odcI* is predominantly upstream from a gene (*potE*) coding for a putrescine-
217 ornithine antiporter, consistently with the function of OdcI that converts Orn to Put. In contrast,
218 OdcC coding genes are located in the vicinity of Fe^{2+}-trafficking protein (*yggX*), a lytic murein
219 transglycosylase (*mltC*) genes, an A/G-specific adenine glycosylase (*mutY*), a tRNA
220 (guanosine(46)-N7)-methyltransferase (*trmB*) and an hypothetical protein. Interestingly, a few
221 horizontal gene transfers of *odcI* occurred from *Proteobacteria* to unrelated *firmicutes*: some
222 *Lactobacillus, Staphylococcus lugdunensis*, and *Megasphaera elsdenii.*

223 LdcI, also called *cadA*, appears to be ancestral in some gammaproteobacterial lineages
224 (*Francisellaceae*, *Aeromonadaceae*, *Vibrionaceae* and *Enterobacteriaceae*, Fig. 4A). Moreover,
225 similar to *odcI*/*odcC*, *ldcC* apparently derived from *ldcI*, and more precisely from a gene
226 duplication that occurred, as for *odcI*, just before the emergence of *Sodalis* (PP = 1, Fig. 3A and

bioRxiv preprint doi: https://doi.org/10.1101/308080; this version posted May 26, 2018. The copyright holder for this preprint (which was not certified by peer review) is the author/funder. All rights reserved. No reuse allowed without permission.

BV = 100%, Fig. 3B, and Fig. 4B). The *ldcI* gene forms the *cadBA* operon together with the lysine-cadaverine antiporter-encoding the *cadB* gene. In *Enterobacteriaceae*, this operon is known to be regulated by the transcriptional factor CadC integrating three external signals – low pH, high lysine and low Cad levels (Kuper & Jung, 2005, Fritz *et al.*, 2009). Our analysis confirmed the conserved genomic organization of the *cadCBA* system (Fig. S2) (Zhao & Houry, 2010) allowing *Enterobacteria* to face acid and oxidative stresses. The *ldcC* genomic context seems to be also strongly conserved (Fig. S2) with genes coding for hydroxymyristol acyl carrier protein dehydratase, UDP-N-acetylglucosamine acetyltransferase, tetraacyldisaccharide-1-P synthase, ribonuclease HII, DNA polymerase III alpha subunit, acetyl-CoA carboxylase 2C alpha subunit upstream and putative lyase and tRNA(Ile)-lysidine synthetase genes downstream.

In sharp contrast with OdcI/OdcC and LdcI/LdcC, the Adc group presents a patchy taxonomic distribution and the relationships among Adc sequences are at odds with current systematics, with sequences from different classes of *Proteobacteria* being intermixed on the tree (Fig. 3B and Fig. 4). This indicates that the Adc subfamily was heavily impacted by horizontal gene transfers. The genomic context of *adc* is not conserved (Fig. S2), precluding identification of potential functional partners. Interestingly, the *Burkholderia* sp. AIU 395 LAOdc that locates in the Adc group was shown to possess a lysine decarboxylase and oxidase activity (Sugawara *et al.*, 2014).

Phylogenetic analyses of LAOdc disclose a fourth group in Proteobacteria

As specified above, beside OdcI/C, LdcI/C and Adc, a fourth group of LAOdc sequences is present in the tree. This group contains LdcA from *P. aeruginosa*, shown to possess a lysine

bioRxiv preprint doi: https://doi.org/10.1101/308080; this version posted May 26, 2018. The copyright holder for this preprint (which was not certified by peer review) is the author/funder. All rights reserved. No reuse allowed without permission.

249 decarboxylase activity (Chou *et al.*, 2010). Homologues of LdcA are found in other
250 *Pseudomonadaceae* and in *Betaproteobacteria*. Both groups of sequences are well separated on
251 the tree and widely distributed in these two taxa, with relationships globally in agreement with
252 the current taxonomy. This suggests that an LdcA homologue was present in the ancestor of
253 *Pseudomonadaceae* and in the ancestor of *Betaproteobacteria* and has been globally well
254 conserved along the diversification of these two taxa. The genetic environment of *ldcA* is not
255 conserved (Fig. S2). To our knowledge, the only publication describing a member of the LdcA
256 subfamily concerns *P. aeruginosa*, a highly versatile bacterium that efficiently grows on arginine
257 but not on lysine (Fothergill & Guest, 1977, Rahman & Clarke, 1980). In this organism exhibiting
258 tightly interconnected lysine and arginine catabolism networks (Chou *et al.*, 2010, Madhuri
259 Indurthi *et al.*, 2016), the *PA1818* gene was identified as a part of the ArgR regulon upon growth
260 on excess arginine, but was surprisingly found to code for a lysine decarboxylase, and not for an
261 arginine decarboxylase as one would have logically supposed, and therefore called *ldcA* (Chou *et*
262 *al.*, 2010, Madhuri Indurthi *et al.*, 2016). *P. aeruginosa* is a major cause of gram-negative
263 infections, especially in patients with compromised and weakened immune system. This
264 opportunistic pathogen is also a well-identified threat for patients suffering from Cystic Fibrosis
265 (CF), because the chronic respiratory infections associated to host inflammatory responses lead
266 to pulmonary tissue destruction and lung failure (Bodey *et al.*, 1983, Gellatly & Hancock, 2013).
267 The occurrence and persistence of *P. aeruginosa* in the CF patients' lungs, whose secretions
268 were shown to be acidified and to become oxidative (Pezzulo *et al.*, 2012), hints to a possible
269 role of LdcA in promoting bacterial fitness. Therefore, in the following sections, we chose to
270 deepen the present knowledge on expression, regulation and functional characterization of *P.*

bioRxiv preprint doi: https://doi.org/10.1101/308080; this version posted May 26, 2018. The copyright holder for this preprint (which was not certified by peer review) is the author/funder. All rights reserved. No reuse allowed without permission.

aeruginosa LdcA.

LdcA expression is growth-phase dependent

To determine the role of the LdcA protein in *P. aeruginosa*, the prerequisite was to know when the protein is produced by the bacterium and what are the mechanisms controlling its production. Thus, we first analyzed the expression of its gene by creating a transcriptional fusion between the *ldcA* promoter (*PldcA*) and the reporter *lacZ* gene. The fusion was then integrated into the chromosome of PAO1 (see Materials and Methods for further details), the first *P. aeruginosa* sequenced strain (Stover *et al.*, 2000) considered as a reference strain and widely studied. We then measured the β-galactosidase activity of the PAO1::P_{ldcA}-*lacZ* strain grown in a minimal medium P (MMP) containing glutamate as a carbon source and lysine or arginine (20mM) as additives. Unlike lysine, arginine was able to induce the expression of *ldcA* in PAO1::P_{ldcA}-*lacZ* (not shown), in agreement with published data identifying ArgR as a positive regulator of *ldcA* expression in the PAO1 strain (Lu *et al.*, 2004, Chou *et al.*, 2010).

The pattern of *ldcA* expression was followed during the growth both in minimal and rich media. In MMP medium supplemented with glutamate and arginine (MMP-GR), the β-galactosidase activity increased slightly but continuously along the growth and reached a maximum in the stationary phase (Fig. 5A). Expression of *ldcA* in LB rich medium followed the same pattern of expression (Fig. 5B), that was paralleled by an increase in LdcA protein amount assessed by western blot (not shown). The expression level obtained in LB was two-fold lower that the one measured in MMP-GR. Addition of 20 mM arginine to LB did not change the growth rate of the bacteria but the *ldcA* promoter activity increased during the transition to the

bioRxiv preprint doi: https://doi.org/10.1101/308080; this version posted May 26, 2018. The copyright holder for this preprint (which was not certified by peer review) is the author/funder. All rights reserved. No reuse allowed without permission.

293 stationary phase to reach a level similar to the one measured in MMP-GR (Fig. 5B), indicating a
294 probable limiting concentration of the amino acid in LB at late growth.
295
296 *LdcA expression differs from that of LdcC and LdcI*
297 The *ldcA* genomic context being different from that of *ldcI* and *ldcC* genes (Fig. S2), we
298 wondered if *ldcA* was also regulated differently than these genes; this knowledge could further
299 provide information on its role in *P. aeruginosa* physiology. Even if *E. coli* LdcC is called
300 "constitutive Lysine Decarboxylase", the corresponding gene was shown to be induced in
301 stationary phase in LB medium by RpoS, the sigma factor of stationary phase (Kikuchi *et al.*,
302 1998). However, *ldcA* expression was not affected in a *rpoS* mutant background (data not
303 shown), in agreement with previous transcriptomic analyses demonstrating that *ldcA* is not part
304 of the RpoS regulon (Schuster *et al.*, 2004). To compare with LdcI, the "inducible Lysine
305 Decarboxylase", despite the absence of a CadC homologue in *P. aeruginosa,* we assessed if acid
306 stress could activate the expression of *ldcA* in a CadC-independent manner. Hence, we induced
307 acid stress by decreasing the pH of the medium to a value of 5 during the exponential phase of
308 growth and documented an absence of effect of this treatment on *ldcA* expression (Fig. S3A). In
309 addition, *ldcI* from *V. vulnificus* was reported to be induced by SoxR upon H_2O_2 stress (Kim *et al.*,
310 2006). In *P. aeruginosa*, SoxR is not a key player in the oxidative stress response, but H_2O_2
311 activates the global regulator OxyR that orchestrates the defense against ROS (Ochsner *et al.*,
312 2000). Yet, addition of 1 mM of H_2O_2 in the culture did not affect *ldcA* expression (Fig. S3A). To
313 conclude, *P. aeruginosa* does not overexpress *ldcA* to respond to low pH or oxidative stress
314 conditions.

bioRxiv preprint doi: https://doi.org/10.1101/308080; this version posted May 26, 2018. The copyright holder for this preprint (which was not certified by peer review) is the author/funder. All rights reserved. No reuse allowed without permission.

315

316 *Low pH survival is not affected in absence of LdcA*

317 To clarify the function of LdcA in *P. aeruginosa,* a mutant deleted of the *ldcA* gene, as
318 well as a complemented strain in which one copy of *ldcA* driven by its own promoter was
319 inserted in the chromosome, were engineered (see Materials and Methods). Using Biolog
320 system, a Phenotype MicroArray analysis was carried out to test a large number of stress
321 conditions in systematical and reproducible manner. A potential role of LdcA in detoxifying and
322 protecting *P. aeruginosa* during acid, alkaline and oxidative stress, antibiotic treatment and toxic
323 molecules causing DNA damage, nitrosative stress, and membrane destabilization was assessed.
324 After monitoring the growth of *P. aeruginosa* in the different conditions in minimal medium
325 during 24 hours (see Materials and Methods), the "Area Under the Curve" (AUC) in each
326 condition was calculated and compared between the strains. Analysis of the growth fitness of
327 wild-type, mutant and complemented strains indicated that *P. aeruginosa* could grow optimally
328 in a pH range from 5 to 10 without considerable effect on the metabolism and biomass growth.
329 At pH 4 to 5, the bacterial growth started to be strongly inhibited and the strains were unable to
330 grow below pH 4 (Fig. S3B). This set of experiments did not show any significant difference
331 between the mutant and the wild-type and complemented strains, pointing to a non-
332 involvement of LdcA in survival at low pH. Similarly, no significant effect of *ldcA* absence on
333 resistance against antibiotics, oxidative and toxic agents could be detected (not shown). Hence
334 LdcA seems not to be important for stress response.

335

336 *The Cad pool generated by LdcA impacts persistence phenotype and polyamine content*

bioRxiv preprint doi: https://doi.org/10.1101/308080; this version posted May 26, 2018. The copyright holder for this preprint (which was not certified by peer review) is the author/funder. All rights reserved. No reuse allowed without permission.

In our quest for deciphering the importance of LdcA in bacterial physiology, we analyzed the role of its product Cad shown to play a fundamental role in *P. aeruginosa* virulence. Indeed, this polyamine was reported to be involved in the persistence of the bacterium which is of importance for its eradication by antibiotics; specifically, Cad production was shown to lead to a reduction of the dormant cells that form an antibiotic-tolerant subpopulation in MH medium (Manuel *et al.*, 2010).

Therefore, to assess the role of LdcA in persistence, we first confirmed the impact of *ldcA* mutation on Cad production in this rich MH medium. To do so, we quantified the intracellular Cad amounts in the bacterial strains by liquid chromatography coupled to high resolution mass spectrometry (LC/HRMS) during early-, mid- and late-exponential growth phases. Cad was completely absent in the *ldcA* mutant and complementation with a wild-type *ldcA* copy restored the metabolite level in the strain, indicating that, in PAO1, this polyamine is produced exclusively through the enzymatic activity of LdcA in this growth condition (Fig. 6). Moreover, the wild-type strain showed an impressive increase (around 25-fold) of Cad concentration during the growth, probably reflecting the *ldcA* expression pattern in rich medium (increase during exponential growth, Fig. 5B).

Then, the impact of *ldcA* on the number of persisters during carbenicillin treatment was assessed. As anticipated, *ldcA* mutant showed a number of persisters significantly higher compared to the wild-type PAO1 and complemented strains (Fig. S4), confirming the importance of LdcA activity in the persistence phenotype.

Interestingly, in parallel to Cad, we also quantified the intracellular concentrations of two other polyamines, Put and Spd, in the wild-type strain and *ldcA* mutant (Fig. 6). While in the

bioRxiv preprint doi: https://doi.org/10.1101/308080; this version posted May 26, 2018. The copyright holder for this preprint (which was not certified by peer review) is the author/funder. All rights reserved. No reuse allowed without permission.

359 wild-type PAO1, the amount of Cad is clearly growth-phase dependent, the amounts of Put and
360 Spd were found to be abundant and constant in the MH medium. Remarkably, inactivation of
361 *ldcA* affected not only the production of Cad but also the amount of intracellular Put and Spd
362 which were reduced by around two-fold in the *ldcA* mutant at late exponential growth. This
363 could either indicate a higher turnover of polyamine metabolism in the *ldcA* mutant or a
364 reduced production of Put and Spd as a compensation for the absence of Cad.
365
366 *Polyamines are important for growth fitness*
367 As mentioned above, LdcA synthesis is induced in minimal MMP medium in presence of
368 arginine. Therefore, we monitored the growth of the *ldcA* mutant in this condition in presence
369 of either lysine, the substrate of LdcA, or Cad, the product of its enzymatic transformation. The
370 observed clear reduction of growth of the *ldcA* mutant highlighted the metabolic role of the
371 enzyme, whereas wild-type growth was restored in the complemented strain (Fig. 7A). Addition
372 of exogenous Cad was sufficient to restore a normal growth in the mutant indicating that the
373 limiting factor was indeed the polyamine product (Fig. 7B). Strikingly, growth was also restored
374 when Put (Fig. 7C) or Spd (Fig. 7D) were added to the growth medium at the same
375 concentrations, indicating that these polyamines can substitute for Cad as a growth factor.
376
377 **Discussion**
378 The present exhaustive phylogenetic analysis of the AAT-fold LAOdcs super-family
379 indicates that wing-less enzymes were ancestral in *Firmicutes*, in agreement with earlier reports
380 (Sekowska *et al.*, 1998, Burrell *et al.*, 2010). This analysis highlights also the ancestral presence

bioRxiv preprint doi: https://doi.org/10.1101/308080; this version posted May 26, 2018. The copyright holder for this preprint (which was not certified by peer review) is the author/funder. All rights reserved. No reuse allowed without permission.

of wing-less AAT-fold LAOdc in *Cyanobacteria*. Yet, no LAOdc activity of a cyanobacterial AAT-fold enzyme has been documented despite their purification from *Anabaena variabilis* and *Nostoc punctiforme* (Burrell *et al.*, 2010). We show that wing domain-containing AAT-fold LAOdc emerged during the diversification of *Proteobacteria*, suggesting that short AAT-fold LAOdc could be more ancient and that the acquisition of the CheY-like wing domain occurred likely secondarily, as previously proposed (Burrell *et al.*, 2010, Kanjee *et al.*, 2011a). The absence of AR-fold decarboxylases in *Firmicutes* (Burrell *et al.*, 2010, Michael, 2016a)implies that their AAT-fold decarboxylases would be the only route for polyamine biosynthesis and thus emphasizes the importance of these enzymes in this phylum. The *Firmicutes* AAT-fold LAOdc correspond to two copies, likely paralogues (A and B), present in most species and easily distinguishable by their genomic context. These two copies result from a duplication event that occurred very early during diversification of the phylum, probably in the ancestor of Clostridia and Bacilli (Fig. S1). Copy A encompasses the *B. subtilis yaaO* (Sekowska *et al.*, 1998), while copy B contains the *B. subtilis speA* gene coding for an arginine decarboxylase (NP_389346.1) (Burrell *et al.*, 2010). Two other *Firmicutes* proteins corresponding to copy B sequences (from *Clostridium difficile* YP_001087362.1 and *S. ruminantium* WP_014425426.1) (Fig. 1A) were also shown to possess an arginine decarboxylase activity (Liao *et al.*, 2008, Burrell *et al.*, 2010), which led to a hypothesis that copy B AAT-fold decarboxylases would be Adcs (Burrell *et al.*, 2010). The function of copy A awaits further investigation and, to our knowledge, the only study focused on the *yaaO* gene (copy A) concluded that in *B. subtilis* this protein had no effect on polyamine production (Sekowska *et al.*, 1998).

Regarding the evolutionary history of the wing domain-containing LAOdcs, our analysis

bioRxiv preprint doi: https://doi.org/10.1101/308080; this version posted May 26, 2018. The copyright holder for this preprint (which was not certified by peer review) is the author/funder. All rights reserved. No reuse allowed without permission.

reveals that proteobacterial LAOdcs form two monophyletic groups, Odc and LAdc. Thus, lysine and arginine decarboxylases appear more closely related to each other than to ornithine decarboxylases, although the relationships among the two Ldc families (LdcI/C and LdcA) and the Adc family are not resolved (PP <0.5) (Fig. 3A). Furthermore, we showed that the proteobacterial biosynthetic OdcC and LdcC emerged from inducible Odc and Ldc (*i.e.* OdcI and LcdI, respectively) through two independent gene duplication events that occurred in *Enterobacteriaceae*, after the divergence of *Sodalis*. Given that both duplication events seem to occur in the same branch of the phylogenetic tree, it is tempting to hypothesize that they are linked, and that a functional connection between both biosynthetic subgroups may have existed. The emergence of biosynthetic enzymes from inducible ones may appear contra-intuitive at the first glance, but may reflect an expansion and a diversification of polyamine functions in these lineages. This would also explain why *Enterobacteriaceae* possess also a constitutive pathway of polyamine synthesis through an AR-fold Adc.

The exhaustive phylogenetic analysis of AAT-fold decarboxylases discloses multiple cases of horizontal gene transfers (e.g. within Cluster III, from *Firmicutes* to *Firmicutes* and to *Actinobacteria* within Cluster I, but also from *Proteobacteria* to *Firmicutes* within cluster II). Interestingly, the two wing-less AAT-fold LAOdc coding genes found in *L. saerimneri* 30a were proposed to result from the horizontal gene transfer of an acid stress inducible Odc from *Enterobacteriaceae*, followed by a gene duplication event (Romano *et al.*, 2013, Romano *et al.*, 2014). One of the two resulting paralogues is thought to have kept the original function (WP_009553942.1), while the other acquired the capacity to use lysine as substrate (EKW98991.1). Instead, our analysis points to a different scenario. In fact, the two copies

bioRxiv preprint doi: https://doi.org/10.1101/308080; this version posted May 26, 2018. The copyright holder for this preprint (which was not certified by peer review) is the author/funder. All rights reserved. No reuse allowed without permission.

present in *L. saerimneri* branch in two different parts of the OdcI tree (Fig. S5), meaning that they have different origins, and result likely from two independent horizontal gene transfer events of OdcI coding genes, whereupon one of these two acquired genes shifted secondarily towards the capacity to use lysine instead of ornithine. Interestingly, the lysine decarboxylating copy is present in various *Lactobacilli*, while the copy using ornithine as substrate is specific to *L. saerimneri* (Fig. S5), suggesting that the former was acquired first. Remarkably, these two enzymes rely on the same antiporter capable to exchange both ornithine/Put and lysine/Cad pairs, resulting in a unique three-component decarboxylation system involved in acid stress response (Romano *et al.*, 2013). This case of substrate specificity shift is probably not an exception, as exemplified by *Burkholderia* sp. AIU 395 in which an AAT-fold enzyme using lysine as substrate branches within the Adc cluster in phylogenetic trees (Fig. 3). Beside substrate shift, existence of dual specificity has been most extensively documented in the case of AR-fold LOdcs, exemplified by bifunctional enzymes of *S. ruminantium* (Takatsuka *et al.*, 2000) and *V. vulnificus* (Lee *et al.*, 2007). In particular, crystal structures of the *V. vulnificus* enzyme in complex with either Put or Cad revealed that the dual substrate specificity is based on a bridging water molecule necessary for the binding of a shorter Put ligand in addition to the longer Cad. A similar dual substrate specificity mechanism may also exist in the case of the AAT-fold LAOdc enzymes although it has not been documented up to now.

Altogether, our data indicate that functional changes affecting gene regulation, substrate fixation, and cellular function occurred several times during the evolution of AAT-fold enzymes. In the light of these observations, one may wonder if the so-called Adc, LdcC, LdcI, OdcC, and OdcI clusters defined according to phylogenetic criteria correspond indeed to homogeneous

bioRxiv preprint doi: https://doi.org/10.1101/308080; this version posted May 26, 2018. The copyright holder for this preprint (which was not certified by peer review) is the author/funder. All rights reserved. No reuse allowed without permission.

447 functional groups and thus if phylogenetic criteria/sequence similarity based measures are good
448 predictors of the function of the AAT-fold enzymes. The very restricted number of
449 experimentally characterized enzymes calls for caution and for the urgent need for additional
450 experimental data.

451 One of the main results of the presented phylogenetic analysis is the identification of a
452 novel large family of decarboxylases, called LdcA, ancestral in *Betaproteobacteria* and in
453 *Pseudomonadaceae*. Thus, the second part of this work was dedicated to functional
454 characterization of the LdcA from a major human opportunistic pathogen *P. aeruginosa*.

455 The *ldcA* gene belongs to the core genome of *P. aeruginosa*, comprising at least 4,000
456 conserved genes (Hilker *et al.*, 2015, Valot *et al.*, 2015). Similarly to *ldcI*, in *P. aeruginosa,*
457 *Pseudomonas resinovorans, Pseudomonas denitrificans* and *Pseudomonas knackmusii, ldcA* is
458 organized in a gene cluster with a gene coding for a homologue of the CadB antiporter,
459 although *cadB* (*PA1819* in *P. aeruginosa*) appears downstream, and not upstream, of the lysine
460 decarboxylase-encoding gene. The presence of a dedicated Lys/Cad transporter could be
461 important from a physiological standpoint because CadB is involved not only in
462 substrate/product exchange but also in the generation of proton motive force
463 (Soksawatmaekhin *et al.*, 2004). Remarkably, the proximity of *cadB* and *ldcA* is an exception in
464 the *ldcA* subfamily (Fig. S2), which does not rule out a hypothesis that LdcA could have another
465 function in other taxa. The whole of our data suggests that LdcI and *P. aeruginosa* LdcA are
466 different in terms of regulation and function. Indeed, we clearly show that LdcA is not involved
467 in acid or oxidative stress response, and its expression is triggered by neither of these stresses;
468 instead it is controlled by ArgR and QS. More similar to LdcC, *P. aeruginosa* LdcA, and certainly

bioRxiv preprint doi: https://doi.org/10.1101/308080; this version posted May 26, 2018. The copyright holder for this preprint (which was not certified by peer review) is the author/funder. All rights reserved. No reuse allowed without permission.

the other members of this novel lysine decarboxylase subfamily, are biosynthetic enzymes responsible for the Cad production by the bacterium.

Importantly, LdcA is the only Cad producing enzyme in *P. aeruginosa* PAO1, as demonstrated by the measurement of the intracellular contents of Cad (Fig. 6). This conclusion was unexpected considering that the product of another gene, *PA4115*, was previously reported to be responsible for 25% of Cad production in overnight cultures grown in the same medium as the one used in our assays, and therefore proposed to be an Ldc (Manuel *et al.*, 2010). After carboxypenicillin treatment, the *PA4115* mutant exhibited an increased number of persisters that was significantly reduced upon addition of exogenous Cad, further supporting the hypothesis of PA4115 being an Ldc (Manuel *et al.*, 2010). Yet, our careful inspection of its sequence revealed that PA4115 belongs to the family of Lonely Guy (LOG) proteins because it contains a highly conserved PGGxGTxxE motif and a nucleotide-binding Rossmann fold. Remarkably, LOG proteins were shown to be often mis-annotated as lysine decarboxylase enzymes, yet without support by biochemical or functional data, whereas they actually possess a cytokinin-specific phosphoribohydrolase activity (Dzurova *et al.*, 2015, Seo & Kim, 2017) or a pyrimidine/purine nucleotide 5'-monophosphate nucleosidase activity (Sevin *et al.*, 2017). Recently, PPnN (or YghD) from *E. coli*, a close homologue sharing 56% identity with PA4115, has been shown to catalyze the hydrolysis of N-glycosidic bond of AMP, GMP, IMP, CMP, dTMP and UMP to form ribose 5-phosphate and the corresponding free base. Hence, it is quite likely that PA4115 catalyzes the same reaction and plays a role in maintaining the nucleotide pool homeostasis by degrading excess nucleotides in *P. aeruginosa* (Sevin *et al.*, 2017). Therefore, the reduced production of Cad in *PA4115* mutant needs to be confirmed because the

bioRxiv preprint doi: https://doi.org/10.1101/308080; this version posted May 26, 2018. The copyright holder for this preprint (which was not certified by peer review) is the author/funder. All rights reserved. No reuse allowed without permission.

relationship between PA4115 and LdcA activity is not clear and could involve indirect causes.

The persistence phenotype observed in *ldcA* mutants is consistent with the beneficial effect of LdcA on growth fitness. Indeed, recent research on bacterial persistence uncovered intracellular ATP concentrations as being one of the major factors affecting the amount of persister cells, and demonstrated that ATP levels are sufficient to predict bacterial tolerance to antibiotics (Conlon *et al.*, 2016, Shan *et al.*, 2017). Considering that Cad produced by LdcA is metabolized and used up by the Krebs cycle to create ATP and that the activity of the lysine/Cad antiporter generates proton motive force essential for ATP synthesis (Soksawatmaekhin *et al.*, 2004), one would expect that in *P. aeruginosa* the *ldcA* mutation may lead to a decrease in ATP levels, which in turn would result in an increase of persisters' population. This hypothesis could be challenged by blocking the Cad degradation pathway or the CadB antiporter activity.

The capacity of Put and Spd to complement the growth phenotype of the *ldcA* mutant and boost *P. aeruginosa* cultures in minimal medium suggests that in *P. aeruginosa* the three major polyamines share certain properties. In the same lines, Cad was shown to substitute for Put and Spd as growth factors in *E. coli* cells depleted of these two polyamines (Igarashi *et al.*, 1986). The growth phenotype described in our work is observed under specific growth conditions. It reveals the importance of Cad when growing *P. aeruginosa* in minimal medium and highlights a certain redundancy in the function of polyamines. It remains to be investigated whether the phenotype is linked to a regulatory effect of Cad or to its anabolism. Recent literature about *Eikenella corrodens* has pointed out the importance of an AAT-fold Ldc (belonging to LdcI group) as a virulence factor against eukaryotic cells that acts through depletion of essential lysine (Lohinai *et al.*, 2015). Therefore the potential role of LdcA in the

bioRxiv preprint doi: https://doi.org/10.1101/308080; this version posted May 26, 2018. The copyright holder for this preprint (which was not certified by peer review) is the author/funder. All rights reserved. No reuse allowed without permission.

513 virulence of *P. aeruginosa* may warrant further investigation. In the present study, we observed
514 that the absence of the enzyme did not affect T3SS-dependent cytotoxicity or the mobility
515 relying on flagellum and Type IV pili (not shown). However, it would also be relevant to probe
516 the importance of LdcA during mouse infection, where the proper functioning of *P. aeruginosa*
517 metabolism is primordial for virulence.

518 Our study reveals that the *ldcA* gene is relatively ancient in *Proteobacteria*, being
519 ancestral in *Betaproteobacteria* and in *Pseudomonadaceae*, two taxa that cover a wide range of
520 ecological niches. Information about regulation and function of an enzyme of the previously
521 unknown LdcA subfamily enables a step further towards understanding of the evolution and the
522 importance of Cad metabolism in bacteria.

523

524 **Experimental procedures**

525

526 *Phylogeny: Dataset assembly*

527 Functionally characterized sequences of AAT-fold LAOdcs were retrieved from NCBI: LdcI
528 (NP_418555.1), LdcC (NP_414728.1), Adc (NP_418541.1), OdcC (NP_417440.1), and OdcI
529 (NP_415220.1) from *E. coli* str. K-12 substr., MG1655 and LdcA (NP_250509.1) from *P.*
530 *aeruginosa* PAO1. These sequences were used as seeds to query a local database containing
531 4,466 complete proteomes of prokaryotes downloaded from the NCBI
532 (ftp://ftp.ncbi.nlm.nih.gov) with the BLASTP 2.2.6 software (Altschul *et al.*, 1997) using default
533 parameters. Homologues of LAODc were retrieved and aligned using MAFFT v7 (Katoh &
534 Standley, 2013). The resulting multiple alignment was used to build a HMM profile with the

bioRxiv preprint doi: https://doi.org/10.1101/308080; this version posted May 26, 2018. The copyright holder for this preprint (which was not certified by peer review) is the author/funder. All rights reserved. No reuse allowed without permission.

HMMbuild program from the HMMER v3.1b1 package (McClure MA, 1996). This profile was then used to query the local database of complete proteomes with the HMMsearch program. Sequences with e-values lower than 2.2e-13 were retrieved. Finally, the search for potential unannotated sequences was performed using TBLASTN 2.2.6 on genomic sequences corresponding to the 4,466 complete proteomes. This led to the identification of 4,090 homologous sequences.

Phylogeny: Phylogenetic inference

To limit taxonomic redundancy for phylogenetic analyses, a sampling of the retrieved sequences by selecting randomly one strain per species has been performed. Multiple alignments were built with MAFFT using the L-INS-i option that allows the construction of accurate multiple alignments and trimmed with BMGE v1.1 with matrix substitution BLOSUM30 (Criscuolo & Gribaldo, 2010).

Maximum likelihood trees were inferred with PhyML 3.1 (Guindon *et al.*, 2010). The best suited evolutionary models were selected using the model test tool implemented in IQ-TREE v1.4.1 according to the Bayesian information criterion (BIC) (Nguyen *et al.*, 2015). The robustness of the inferred trees was assessed using the non-parametric bootstrap procedure implemented in PhyML (100 replicates of the original datasets). Bayesian trees were inferred using MrBayes v3.2.6 (Ronquist & Huelsenbeck, 2003). Two runs were launched with four chains for each run (50,000 iterations). The first 25% of the trees were discarded as burn-in and chain convergence has been checked by analysing the evolution of the Ln(L) curve and checking the average standard deviation of split frequencies values. Figures of trees have been generated using

bioRxiv preprint doi: https://doi.org/10.1101/308080; this version posted May 26, 2018. The copyright holder for this preprint (which was not certified by peer review) is the author/funder. All rights reserved. No reuse allowed without permission.

EvolView (He *et al.*, 2016) (http://nar.oxfordjournals.org/content/44/W1/W236) and iTOL (Letunic & Bork, 2016). Genomic context figures have been generated using GeneSpy (https://lbbe.univ-lyon1.fr/GeneSpy/) developed by P.S. Garcia.

Reference phylogenies of *Firmicutes*, *Cyanobacteria, Proteobacteria*, and Enterobacteriaceae strains contained in our local database were inferred using ribosomal proteins as suggested elsewhere (Ramulu *et al.*, 2014). The reference tree of *Firmicutes* has been rooted according to a recent study (Antunes *et al.*, 2016). The reference tree of *Cyanobacteria* has been rooted by including ribosomal protein sequences from *Natranaerobius thermophilus (Firmicutes*) and *Streptomyces albulus (Actinobacteria*). The reference tree of *Proteobacteria* has been rooted according to Gupta (Gupta, 2000). Finally, the reference phylogeny of *Enterobacteriaceae* has been rooted using with *Shewanella baltica* (*Alteromonadales*) and *Pasteurella multocida* (*Pasteurellales*) ribosomal protein sequences.

For each analysis, the ribosomal protein sequences were identified using the RiboDB database engine (Jauffrit *et al.*, 2016) and aligned with MAFFT using the L-INS-i option. The resulting multiple alignments were trimmed as described above and combined to build a large supermatrix that was used to build maximum likelihood phylogenetic trees.

Bacterial strains, plasmids, and growth conditions

The bacterial strains and plasmids used in this study are listed in Table S1 in the supplemental material. Bacteria were cultivated aerobically at 37°C in rich Lysogeny Broth (LB) medium, in Mueller Hinton II (Becton Dickinson) or in minimal medium P (30mM Na_2HPO_4, 14 mM KH_2PO_4, 20mM $(NH4)_2SO_4$, 1 mM $MgSO_4$, 4µM $FeSO_4$, 0.4 µM Pyridoxal-5'-phosphate, pH 7.4) (Haas *et*

bioRxiv preprint doi: https://doi.org/10.1101/308080; this version posted May 26, 2018. The copyright holder for this preprint (which was not certified by peer review) is the author/funder. All rights reserved. No reuse allowed without permission.

579 *al.*, 1977) containing the indicated carbon and nitrogen sources. *P. aeruginosa* was also cultured
580 on Pseudomonas Isolation Agar plates (PIA; Difco). When required, antibiotics were added at
581 the following concentrations (in µg/ml): 100 (ampicillin), 25 (gentamycin), 25 (kanamycin) and
582 10 (tetracycline) for *E. coli*, 200 (carbenicillin), 200 (gentamycin) and 200 (tetracycline) for *P.*
583 *aeruginosa*.
584
585 *Genetic manipulations*
586 To delete *ldcA* gene, fused uspstream and downstream flanking regions of the gene were
587 generated by "Splicing by Overlap Extension" (SOE)-PCR using PAO1 genomic DNA as matrix and
588 appropriate primer pairs. The resulting fragment of 819 bp was cloned into pCR-Blunt II-TOPO
589 vector, sequenced and then subcloned into *Bam*HI-*Hin*dIII sites of pEXG2, leading to
590 pEXG2Δ*ldcA*. The suicide plasmid carries the counter-selectable *sacB* marker from *B. subtilis*
591 which confers sensitivity to sucrose. The plasmid was mobilized into *P. aeruginosa* strain by
592 triparental mating, using the conjugative properties of the helper plasmid pRK2013. Co-
593 integration events were selected on PIA plates containing gentamycin. Single colonies were then
594 plated on PIA medium containing 5% (w/v) sucrose to select for the loss of plasmid: the
595 resulting sucrose-resistant strains were checked for antibiotic sensitivity and for *ldcA* (wild-type
596 or truncated gene) genotype by PCR.
597 To complement the *ldcA* mutant, a 2785 bp-long fragment encompassing the coding
598 sequence and 495 bases upstream the ATG was PCR amplified from PAO1 genomic DNA using
599 appropriate primer pairs. The PCR product was cloned into pCR-Blunt II-TOPO and sequenced.
600 The *Spe*I restriction fragment was subcloned in mini-CTX1 cut with the same enzyme, leading to

bioRxiv preprint doi: https://doi.org/10.1101/308080; this version posted May 26, 2018. The copyright holder for this preprint (which was not certified by peer review) is the author/funder. All rights reserved. No reuse allowed without permission.

601 miniCTX-*ldcA*. A mini-CTX derivative was used to construct a *lacZ* reporter vector. PCR
602 amplification was used to produce the 548 bp-long *ldcA* promoter fragment (-498/+44 relative
603 to translation initiation) with appropriate primers. After ligation into pCR-Blunt II-TOPO vector
604 and sequencing, the fragment was sub-cloned into the *Xho*I-*Eco*RI sites of mini-CTX-lacZ. Both
605 miniCTX-*ldcA* and mini-CTX-*PldcA-lacZ* were introduced into *P. aeruginosa* by triparental
606 conjugation and the transconjugants were selected on PIA plates containing tetracycline. The
607 pFLP2 plasmid was then used to excise the FRT cassette as described (Hoang *et al.*, 1998).
608 Plasmids and primers used in PCR are listed in the Tables S1 and S2, respectively.
609
610 *β-Galactosidase assays*
611 Bacteria were grown aerobically at 37°C in 100 ml flasks with agitation (300 rpm). At the
612 indicated OD, β-galactosidase activity was assayed as described (Miller, 1972), with details
613 reported in (Thibault *et al.*, 2009).
614
615 *Intracellular metabolite analysis*
616 Strains were first isolated from an overnight solid culture at 37°C on Mueller Hinton II agar 1.5%.
617 Precultures and cultures were performed on a Minitron II rotary shaker at 220 rpm (Infors HT)
618 under aerobic conditions (10% of total volume of Erlenmeyer flask). A few bacterial colonies
619 from the agar plate were precultured overnight at 37°C and an aliquot was withdrawn and
620 diluted to an OD_{600} of ~0.1 in a fresh culture medium for the culture step. Growth curves were
621 determined for each strain and used to determine their respective concentration (CFU/ml) and
622 the OD at which the bacteria should be harvested to correspond to early-, mid-, and late-

bioRxiv preprint doi: https://doi.org/10.1101/308080; this version posted May 26, 2018. The copyright holder for this preprint (which was not certified by peer review) is the author/funder. All rights reserved. No reuse allowed without permission.

623 exponential phases.

624 The protocol of the intracellular metabolites sampling was adapted from a previously
625 described procedure (Aros-Calt *et al.*, 2015). In brief, a 5 ml aliquot of cell culture broth was
626 taken from the main culture and was filtered in a few seconds using poly(ether sulfone) sterile
627 membrane disc filters (Supor450, 0.45 µm pore size, PALL) mounted on a Millipore filtration
628 device (Darmstadt). The bacteria on the filter were quickly washed with 5 ml of 0.6% NaCl
629 solution maintained at room temperature. The filter was then rapidly transferred to a 50 ml
630 Falcon tube containing 5 ml of cold 60% ethanol (v/v, ≤ −20°C). The Falcon tube was
631 subsequently quickly immersed in liquid nitrogen. Following this quenching step, tubes
632 containing bacteria on filters in the extraction solution were vortexed 10 times on ice to remove
633 the cells from the filter. Then, a 1 ml aliquot of the cell suspension was transferred to 2 ml tubes
634 containing 0.1 mm glass beads (Bertin Technologies). Cell disruption was performed by three
635 cycles in a Precellys 24 homogenizer (Bertin Technologies) for 30 s at 3,800 rpm at ~4°C. The
636 glass beads and cell debris were separated from the supernatant by centrifugation for 5 min at
637 4°C and 10,000g. A 400 µL aliquot of the supernatant was withdrawn and further vacuum-dried
638 using a SpeedVac instrument (Thermo Fisher Scientific) and stored at −80°C until analysis. Dried
639 extracts were dissolved in an adjusted volume of 95% mobile phase A / 5% mobile phase B to
640 obtain the equivalent of 1.25 10^7 CFU in 15µl before analysis by LC/HR-MS.
641 To detect intracellular metabolites, LC/HR-MS experiments were performed using a Dionex
642 Ultimate chromatographic system (Thermo Fisher Scientific) coupled to an Exactive (Orbitrap)
643 mass spectrometer from Thermo Fisher Scientific fitted with an electrospray source. The mass
644 spectrometer was externally calibrated before each analysis using the manufacturer's

bioRxiv preprint doi: https://doi.org/10.1101/308080; this version posted May 26, 2018. The copyright holder for this preprint (which was not certified by peer review) is the author/funder. All rights reserved. No reuse allowed without permission.

predefined methods and recommended calibration mixture provided by the manufacturer. Chromatographic separation was performed on a Discovery HS F5 PFPP 5 µm, 2.1 × 250 mm column (Sigma) at 30°C. The chromatographic system was equipped with an on-line pre-filter (Thermo Fisher Scientifics). Mobile phases were 100% water (A) and 100% ACN (B), both of which containing 0.1% formic acid. Chromatographic elution was achieved with a flow rate of 250 µl/min. After injection 15 µl of sample, elution started with an isocratic step of 2 min at 5% phase B, followed by a linear gradient from 5 to 100% of phase B in 18 min. These proportions were kept constant for 4 min before returning to 5% of phase B and letting the system equilibrate for 6 min. The column effluent was directly introduced into the electrospray source of the mass spectrometer, and analyses were performed in the positive ion mode. Source parameters were as follows: capillary voltage set at 5 kV; capillary temperature at 300°C; sheath and auxiliary gas (nitrogen) flow rates at 50 and 25 arbitrary units, respectively; mass resolution power of the analyzer set at 50,000 at m/z 200 (full width at half maximum, FWHM) for singly charged ions. The acquisition was achieved from m/z 50 to 250 in the positive ionization mode during the first 12 min of the run. Under these conditions were achieved a good separation and detection (with an average mass accuracy better than 3ppm) of the targeted molecules (under their $[M+H]^+$ form). These species were readily identified in the extracts through the use of the corresponding commercial molecules obtained from Sigma-Aldrich. Extracted ion chromatograms were generated and resulting peaks integrated using the Xcalibur software (version 2.1, Thermo Fisher Scientific) for Spd ($[M+H]^+$ at theoretical m/z 146.1652, retention time 5.24 min), Put (m/z 89.1073, 3.63 min) and Cad (m/z 103.1230, 3.94 min).

bioRxiv preprint doi: https://doi.org/10.1101/308080; this version posted May 26, 2018. The copyright holder for this preprint (which was not certified by peer review) is the author/funder. All rights reserved. No reuse allowed without permission.

Acknowledgments: We thank Rémi Peyraud and Ina Attrée for helpful discussions. This work has received funding from GRAL (ANR-10-LABX-49-01), the European Union's Horizon 2020 research and innovation programme under grant agreement No 647784, and the ANR-16-CE02-0005. This work was also supported by CEA and the French Ministry of Research and National Research Agency as part of the French metabolomics and fluxomics infrastructure (MetaboHUB, ANR-11-INBS-0010 grant). Diego Carriel was supported by a PhD grant from LABEX GRAL and Pierre S. Garcia was supported by a grant from the ARC Santé from the Region Auvergne Rhône-Alpes.

Author contributions: DCL, PSG, FC, and PL performed experiments. All authors analyzed data. IG, SE and CBA designed and supervised the overall study and wrote the paper with contribution from all authors.

Abbreviated Summary

Bacterial polyamines are involved in many fundamental processes and are mainly synthetized by dedicated lysine, arginine and ornithine decarboxylases or LAOdcs. Our exhaustive phylogenetic analysis reveals evolutionary history of LAOdcs and discloses a hitherto overlooked LdcA subfamily. We show that LdcA is playing an important role in growth and persistence of the major multidrug resistant human pathogen *P. aeruginosa*, exerted through cadaverine biosynthesis and concomitant regulation of intracellular levels of putrescine and spermidine.

Figure legends

bioRxiv preprint doi: https://doi.org/10.1101/308080; this version posted May 26, 2018. The copyright holder for this preprint (which was not certified by peer review) is the author/funder. All rights reserved. No reuse allowed without permission.

FIG 1. LAOdcs are ancestral in *Firmicutes*.

(A) Unrooted maximum likelihood phylogeny of LAOdc Cluster I (PhyML, LG+I+G4, 504 sequences, 295 amino-acid positions), displayed as a cladogram. The corresponding phylogram is available at the newick format as supplementary data. Leave colors correspond to taxonomic groups (*Firmicutes*: red, *Cyanobacteria*: green, *Actinobacteria*: yellow, other: grey). External colored rings correspond to copy A (blue) and B (pink). LAOdc sequences discussed in the text or for which functional information is available are indicated with gray arrows. Red dots correspond to bootstrap values (BV). The size of the dots is proportional to BV.

(B) Taxonomic distribution of AAT-fold LAOdc according to a reference maximum likelihood phylogeny of *Firmicutes*, displayed as a cladogram. The corresponding phylogram is available at the newick format as supplementary data. The reference tree was inferred using ribosomal protein sequences (PhyML, LG+I+G4, 38 sequences, 6,133 amino-acid positions) and rooted according to a recent study by Antunes *et al*. (Antunes *et al.*, 2016) Red dots correspond to bootstrap values (BV). The size of the dots is proportional to BV. The blue diamonds pinpoint the emergence of copy A and copy B. Rectangles at leaves indicate that at least one genome of the considered taxon encodes one or more AAT-fold LAOdc. More precisely a green rectangle indicates that the ancestor of the taxon likely contains one (or more) AAT-fold LAOdc gene, while a red rectangle indicates that some members of the taxon acquired secondarily their AAT-fold LAOdc by horizontal gene transfer.

(C) Genomic context of LAOdc A and B in a sample of *Firmicutes*. Black arrows: LAOdc coding genes, colored arrows: conserved neighbor genes.

bioRxiv preprint doi: https://doi.org/10.1101/308080; this version posted May 26, 2018. The copyright holder for this preprint (which was not certified by peer review) is the author/funder. All rights reserved. No reuse allowed without permission.

FIG 2. LAOdcs are ancestral in *Cyanobacteria*.

(A) Maximum likelihood phylogeny of LAOdc of *Cyanobacteria* (PhyML, LG+I+G4, 28 sequences, 446 amino-acid positions), displayed as a cladogram. The corresponding phylogram is available at the newick format as supplementary data. The tree has been rooted according to the reference phylogeny of *Cyanobacteria* (see above). Leave colors correspond to taxonomic groups. Red dots correspond to bootstrap values (BV). The size of the dots is proportional to BV.

(B) Taxonomic distribution of AAT-fold LAOdc according to a reference maximum likelihood phylogeny of *Cyanobacteria*, displayed as a cladogram. The corresponding phylogram is available at the newick format as supplementary data. The reference tree was inferred using ribosomal protein sequences (PhyML, LG+I+G4, 30 sequences, 6,394 amino acid positions). The tree has been rooted using sequences from *Firmicutes* (*Natranaerobius thermophilus*) and *Actinobacteria* (*Streptomyces albulus*). Red dots correspond to bootstrap values (BV). The size of the dots is proportional to BV. The blue diamond pinpoints the origin of AAT-fold LAOdc in *Cyanobacteria*. Rectangles at leaves indicate that at least one genome of the considered taxon encodes one or more AAT-fold LAOdc. More precisely a green rectangle indicates that the ancestor of the taxon likely contains one (or more) AAT-fold LAOdc gene.

(C) Genomic context of LAOdc in a sample of *Cyanobacteria*. Black arrows: LAOdc genes.

Fig. 3. Phylogeny of the LAOdc Cluster II

(A) Bayesian phylogeny of cluster II inferred from a sample of representative sequences and rooted with a sample of sequences from clusters I and III (MrBayes, mixed model+G4, 54

bioRxiv preprint doi: https://doi.org/10.1101/308080; this version posted May 26, 2018. The copyright holder for this preprint (which was not certified by peer review) is the author/funder. All rights reserved. No reuse allowed without permission.

sequences, 392 amino acid positions). The scale bar represents the average number of substitutions per site. Numbers at branches correspond to posterior probabilities. The ML tree inferred with the same dataset supported the same topology (see supplementary data).

(B) Maximum likelihood phylogeny of the LAOdc Cluster II (PhyML, LG+I+G4, 551 sequences, 589 amino-acid positions), displayed as a cladogram. The corresponding phylogram is available at the newick format as supplementary data. LAOdc sequences from *E. coli* and *P. aeruginosa* discussed in the text are indicated with gray arrows. The tree has been rooted according to (A). Colors on the external circle correspond to taxonomic groups: dark blue: *Proteobacteria*, red: *Firmicutes*, yellow: *Actinobacteria*, gray: other taxa. Red dots correspond to bootstrap values (BV). The size of the dots is proportional to BV.

Fig. 4. Taxonomic distribution of LAOdcs in *Proteobacteria*

(A) Taxonomic distribution of AAT-fold LAOdc according to a reference maximum likelihood phylogeny of *Proteobacteria*, displayed as a cladogram. The corresponding phylogram is available at the newick format as supplementary data. The reference tree was inferred using ribosomal protein sequences (PhyML, LG+I+G4, 108 sequences, 6,129 amino acid positions). The tree has been rooted in the branch separating *Deltaproteobacteria* and *Epsilonproteobacteria* in agreement with the study by Gupta (Gupta, 2000). Leave colors correspond to taxonomic groups. Red dots correspond to bootstrap values (BV). The size of the dots is proportional to BV. A blue diamond indicates the ancestral presence of LAOdc families in the corresponding taxon. Rectangles at leaves indicate that at least one genome of the considered taxon encodes one or more AAT-fold LAOdc. More precisely a green rectangle indicates that the ancestor of the taxon

bioRxiv preprint doi: https://doi.org/10.1101/308080; this version posted May 26, 2018. The copyright holder for this preprint (which was not certified by peer review) is the author/funder. All rights reserved. No reuse allowed without permission.

likely contains one (or more) AAT-fold LAOdc gene, while a red rectangle indicates that some members of the taxon acquired secondarily their AAT-fold LAOdc by horizontal gene transfer. (B) Taxonomic distribution of AAT-fold LAOdc according to a reference maximum likelihood phylogeny of *Enterobacteraceae*, displayed as a cladogram. The corresponding phylogram is available at the newick format as supplementary data. The reference tree was inferred using ribosomal protein sequences (PhyML, LG+I+G4, 34 sequences, 6,333 amino acid positions). The tree was rooted with *Shewanella baltica* (*Alteromonadales*) and *Pasteurella multocida* (*Pasteurellales*). Leave colors correspond to taxonomic groups. Other legend elements are identical to (A).

Fig. 5. Factors influencing *ldcA* expression

Activity of *ldcA* promoter fused to *lacZ* reporter gene was assessed during growth in different media and genetic backgrounds. Measurements of the β-galactosidase activity of PAO1*::PldcA-lacZ* strain grown either in minimal medium P (MMP) containing 20 mM L-glutamate and 20 mM arginine (A), or in LB containing or not 20 mM arginine (B) were performed at times indicated. C. β-galactosidase activity of wild-type and indicated mutant CHA strains harboring the *PldcA-lacZ* fusion and grown in LB. β-galactosidase activity is expressed in Miller Units (left Y-axis) and presented in the bar graphs. Growth was performed in 125 ml flasks, followed by measure of OD_{600} (right Y-axis) and plotted on lines. Results are the average of values from three independent experiments ± standard deviation (SD).

Fig. 6. Intracellular Cad in rich medium is produced by the lysine decarboxylase LdcA

bioRxiv preprint doi: https://doi.org/10.1101/308080; this version posted May 26, 2018. The copyright holder for this preprint (which was not certified by peer review) is the author/funder. All rights reserved. No reuse allowed without permission.

A. Growth curves of the wild-type strain, the *ldcA* mutant and the complemented strain in the rich Mueller Hinton medium.

B. Intracellular concentration, expressed in area of chromatogram peak, of the three indicated polyamines at (1) early-, (2) mid- and (3) late-exponential growth phases as indicated.

Fig. 7. Polyamines are important for growth fitness in minimal medium

Growth of the wild-type PAO1 strain, the *ldcA* mutant and the complemented strain in minimal MMP medium supplemented with 20 mM glutamate, 1mM arginine and 5 mM of (A) lysine, (B) Cad, (C) Put or (D) Spd in 96-well plates. The experiments are representative of two experiments.

Supporting informations

Supplemental material and methods

Fig. S1. AAT-fold LAOdc are widespread in *Bacteria*

(A) Taxonomic distribution of AAT-fold LAOdc in prokaryotes. For each phylum and class, ratio corresponds to the number of proteomes containing at least one homologue on the number of proteomes present in our database. Taxa represented by at least 10 proteomes, among which more than 20% contained at least one AAT-fold LAOdc homologue are highlighted by colors.

(B) Unrooted ML tree of AAT-fold LAOdcs (PhyML, LG+I+G4, 1,117 sequences, 273 amino-acid positions). The tree can be divided in three parts: Cluster I corresponds to wing-less LAOdc mainly from *Firmicutes*, *Actinobacteria* and *Cyanobacteria*; Cluster II encompasses wing domain

bioRxiv preprint doi: https://doi.org/10.1101/308080; this version posted May 26, 2018. The copyright holder for this preprint (which was not certified by peer review) is the author/funder. All rights reserved. No reuse allowed without permission.

799 containing LAOdc mainly from *Proteobacteria,* while Cluster III gathers wing-less and wing
800 domain-containing LAOdc from various and unrelated taxa. The scale bar represents the
801 number of substitutions per site. Bootstrap values (BV) associated to branches separating the
802 three clusters are indicated.
803
804 **Fig. S2.** Genomic context of LAOdc genes from Cluster II
805 Genomic context of LdcC, LdcI, OdcC, OdcI, Adc, and Ladc coding genes in a sample of
806 Proteobacteria. Black arrows: LAOdc coding genes, colored arrows: conserved neighbor genes.
807
808 **FIG S3** Influence of stress on *ldcA* expression and growth fitness of *P. aeruginosa.* (A) Effect of
809 acid and oxidative stress during growth in rich medium. At T_0, HCl was added to shift the pH of
810 LB medium from neutral to pH 5 while H_2O_2 was added to a final entration of 1mM. β-
811 galactosidase activity of PAO1*::PldcA-lacZ* strain was measured at T_0, then monitored 30 and 60
812 min after treatment. B) Growth of PAO1 in minimal medium at different pHs was evaluated
813 using Biolog high-throughput system. Each point corresponds to the "Area Under the Curve"
814 (AUC) measured after 24h of bacterial growth.
815
816 **FIG S4** LdcA function affects carbenicillin persistence. Percentage of survivors in rich medium
817 (cation-adjusted Mueller Hinton Broth) after 24h of carbenicillin treatment. Growth was
818 performed in erlenmeyer flasks at 37°C with agitation (300 RPM). Percentage of survivors was
819 calculated from CFU counting after 24h of antibiotic treatment at 500µg/ml (8X MIC).
820

bioRxiv preprint doi: https://doi.org/10.1101/308080; this version posted May 26, 2018. The copyright holder for this preprint (which was not certified by peer review) is the author/funder. All rights reserved. No reuse allowed without permission.

FIG. S5 Maximum likelihood tree of OdcI/OdcC sequences (in blue) (PhyML, LG+I+G4, 514 sequences, 583 amino-acid positions), disclosing the proteobacterial origin of the OdcI sequences reported by previous studies in a few firmicutes (in dark red) (Romano *et al.*, 2013, Romano *et al.*, 2014). These sequences were likely acquired through at least three horizontal gene transfers indicated by dark yellow branches. The tree was rooted with Adc (orange triangle), LdcA (green triangle), and LdcI/C (blue triangle) sequences. The pink triangle correspond to OdcC sequences. Numbers at branches correspond to aLRT supports. The scale bar indicates the average number of substitutions per site.

Table S1 List of bacterial strains and plasmids used in this work.

Table S2 Primers used in this study.

REFERENCES

Altschul, S.F., T.L. Madden, A.A. Schaffer, J. Zhang, Z. Zhang, W. Miller & D.J. Lipman, (1997) Gapped BLAST and PSI-BLAST: a new generation of protein database search programs. *Nucleic Acids Res* **25**: 3389-3402.

Antunes, L.C., D. Poppleton, A. Klingl, A. Criscuolo, B. Dupuy, C. Brochier-Armanet, C. Beloin & S. Gribaldo, (2016) Phylogenomic analysis supports the ancestral presence of LPS-outer membranes in the Firmicutes. *Elife* **5**.

Aros-Calt, S., B.H. Muller, S. Boudah, C. Ducruix, G. Gervasi, C. Junot & F. Fenaille, (2015) Annotation of the Staphylococcus aureus Metabolome Using Liquid Chromatography Coupled to High-Resolution Mass Spectrometry and Application to the Study of Methicillin Resistance. *J Proteome Res* **14**: 4863-4875.

Bodey, G.P., R. Bolivar, V. Fainstein & L. Jadeja, (1983) Infections caused by Pseudomonas aeruginosa. *Rev Infect Dis* **5**: 279-313.

Bunsupa, S., K. Katayama, E. Ikeura, A. Oikawa, K. Toyooka, K. Saito & M. Yamazaki, (2012) Lysine decarboxylase catalyzes the first step of quinolizidine alkaloid biosynthesis and coevolved with alkaloid production in leguminosae. *Plant Cell* **24**: 1202-1216.

bioRxiv preprint doi: https://doi.org/10.1101/308080; this version posted May 26, 2018. The copyright holder for this preprint (which was not certified by peer review) is the author/funder. All rights reserved. No reuse allowed without permission.

Burrell, M., C.C. Hanfrey, L.N. Kinch, K.A. Elliott & A.J. Michael, (2012) Evolution of a novel lysine decarboxylase in siderophore biosynthesis. *Mol Microbiol* **86**: 485-499.

Burrell, M., C.C. Hanfrey, E.J. Murray, N.R. Stanley-Wall & A.J. Michael, (2010) Evolution and multiplicity of arginine decarboxylases in polyamine biosynthesis and essential role in Bacillus subtilis biofilm formation. *J Biol Chem* **285**: 39224-39238.

Chou, H.T., M. Hegazy & C.D. Lu, (2010) L-lysine catabolism is controlled by L-arginine and ArgR in Pseudomonas aeruginosa PAO1. *J Bacteriol* **192**: 5874-5880.

Conlon, B.P., S.E. Rowe, A.B. Gandt, A.S. Nuxoll, N.P. Donegan, E.A. Zalis, G. Clair, J.N. Adkins, A.L. Cheung & K. Lewis, (2016) Persister formation in Staphylococcus aureus is associated with ATP depletion. *Nat Microbiol* **1**: 16051.

Criscuolo, A. & S. Gribaldo, (2010) BMGE (Block Mapping and Gathering with Entropy): a new software for selection of phylogenetic informative regions from multiple sequence alignments. *BMC Evol Biol* **10**: 210.

Dela Vega, A.L. & A.H. Delcour, (1996) Polyamines decrease Escherichia coli outer membrane permeability. *J Bacteriol* **178**: 3715-3721.

Di Martino, M.L., R. Campilongo, M. Casalino, G. Micheli, B. Colonna & G. Prosseda, (2013) Polyamines: emerging players in bacteria-host interactions. *Int J Med Microbiol* **303**: 484-491.

Dzurova, L., F. Forneris, S. Savino, P. Galuszka, J. Vrabka & I. Frebort, (2015) The three-dimensional structure of "Lonely Guy" from Claviceps purpurea provides insights into the phosphoribohydrolase function of Rossmann fold-containing lysine decarboxylase-like proteins. *Proteins* **83**: 1539-1546.

El Bakkouri, M., I. Gutsche, U. Kanjee, B. Zhao, M. Yu, G. Goret, G. Schoehn, W.P. Burmeister & W.A. Houry, (2010) Structure of RavA MoxR AAA+ protein reveals the design principles of a molecular cage modulating the inducible lysine decarboxylase activity. *Proc Natl Acad Sci U S A* **107**: 22499-22504.

Eliot, A.C. & J.F. Kirsch, (2004) Pyridoxal phosphate enzymes: mechanistic, structural, and evolutionary considerations. *Annu Rev Biochem* **73**: 383-415.

Fothergill, J.C. & J.R. Guest, (1977) Catabolism of L-lysine by Pseudomonas aeruginosa. *J Gen Microbiol* **99**: 139-155.

Fritz, G., C. Koller, K. Burdack, L. Tetsch, I. Haneburger, K. Jung & U. Gerland, (2009) Induction kinetics of a conditional pH stress response system in Escherichia coli. *J Mol Biol* **393**: 272-286.

Gale, E.F. & H.M. Epps, (1944) Studies on bacterial amino-acid decarboxylases: 1. l(+)-lysine decarboxylase. *Biochem J* **38**: 232-242.

Gale, E.F. & W.E. Van Heyningen, (1942) The effect of the pH and the presence of glucose during growth on the production of alpha and theta toxins and hyaluronidase by Clostridium welchii. *Biochem J* **36**: 624-630.

Gellatly, S.L. & R.E. Hancock, (2013) Pseudomonas aeruginosa: new insights into pathogenesis and host defenses. *Pathog Dis* **67**: 159-173.

Guindon, S., J.F. Dufayard, V. Lefort, M. Anisimova, W. Hordijk & O. Gascuel, (2010) New algorithms and methods to estimate maximum-likelihood phylogenies: assessing the performance of PhyML 3.0. *Syst Biol* **59**: 307-321.

Gupta, R.S., (2000) The phylogeny of proteobacteria: relationships to other eubacterial phyla and eukaryotes. *FEMS Microbiol Rev* **24**: 367-402.

Haas, D., B.W. Holloway, A. Schambock & T. Leisinger, (1977) The genetic organization of arginine biosynthesis in Pseudomonas aeruginosa. *Mol Gen Genet* **154**: 7-22.

bioRxiv preprint doi: https://doi.org/10.1101/308080; this version posted May 26, 2018. The copyright holder for this preprint (which was not certified by peer review) is the author/funder. All rights reserved. No reuse allowed without permission.

He, Z., H. Zhang, S. Gao, M.J. Lercher, W.H. Chen & S. Hu, (2016) Evolview v2: an online visualization and management tool for customized and annotated phylogenetic trees. *Nucleic Acids Res* **44**: W236-241.

Hilker, R., A. Munder, J. Klockgether, P.M. Losada, P. Chouvarine, N. Cramer, C.F. Davenport, S. Dethlefsen, S. Fischer, H. Peng, T. Schonfelder, O. Turk, L. Wiehlmann, F. Wolbeling, E. Gulbins, A. Goesmann & B. Tummler, (2015) Interclonal gradient of virulence in the Pseudomonas aeruginosa pangenome from disease and environment. *Environ Microbiol* **17**: 29-46.

Hoang, T.T., R.R. Karkhoff-Schweizer, A.J. Kutchma & H.P. Schweizer, (1998) A broad-host-range Flp-FRT recombination system for site-specific excision of chromosomally-located DNA sequences: application for isolation of unmarked Pseudomonas aeruginosa mutants. *Gene* **212**: 77-86.

Igarashi, K. & K. Kashiwagi, (2006) Polyamine Modulon in Escherichia coli: genes involved in the stimulation of cell growth by polyamines. *J Biochem* **139**: 11-16.

Igarashi, K. & K. Kashiwagi, (2015) Modulation of protein synthesis by polyamines. *IUBMB Life* **67**: 160-169.

Igarashi, K., K. Kashiwagi, H. Hamasaki, A. Miura, T. Kakegawa, S. Hirose & S. Matsuzaki, (1986) Formation of a compensatory polyamine by Escherichia coli polyamine-requiring mutants during growth in the absence of polyamines. *J Bacteriol* **166**: 128-134.

Jauffrit, F., S. Penel, S. Delmotte, C. Rey, D.M. de Vienne, M. Gouy, J.P. Charrier, J.P. Flandrois & C. Brochier-Armanet, (2016) RiboDB Database: A Comprehensive Resource for Prokaryotic Systematics. *Mol Biol Evol* **33**: 2170-2172.

Kamio, Y. & K. Nakamura, (1987) Putrescine and cadaverine are constituents of peptidoglycan in Veillonella alcalescens and Veillonella parvula. *J Bacteriol* **169**: 2881-2884.

Kamio, Y., H. Poso, Y. Terawaki & L. Paulin, (1986) Cadaverine covalently linked to a peptidoglycan is an essential constituent of the peptidoglycan necessary for the normal growth in Selenomonas ruminantium. *J Biol Chem* **261**: 6585-6589.

Kandiah, E., D. Carriel, J. Perard, H. Malet, M. Bacia, K. Liu, S.W. Chan, W.A. Houry, S. Ollagnier de Choudens, S. Elsen & I. Gutsche, (2016) Structural insights into the Escherichia coli lysine decarboxylases and molecular determinants of interaction with the AAA+ ATPase RavA. *Sci Rep* **6**: 24601.

Kang, I.H., J.S. Kim, E.J. Kim & J.K. Lee, (2007) Cadaverine protects Vibrio vulnificus from superoxide stress. *J Microbiol Biotechnol* **17**: 176-179.

Kanjee, U., I. Gutsche, E. Alexopoulos, B. Zhao, M. El Bakkouri, G. Thibault, K. Liu, S. Ramachandran, J. Snider, E.F. Pai & W.A. Houry, (2011a) Linkage between the bacterial acid stress and stringent responses: the structure of the inducible lysine decarboxylase. *EMBO J* **30**: 931-944.

Kanjee, U., I. Gutsche, S. Ramachandran & W.A. Houry, (2011b) The enzymatic activities of the Escherichia coli basic aliphatic amino acid decarboxylases exhibit a pH zone of inhibition. *Biochemistry* **50**: 9388-9398.

Kanjee, U. & W.A. Houry, (2013) Mechanisms of acid resistance in Escherichia coli. *Annu Rev Microbiol* **67**: 65-81.

Karatan, E. & A.J. Michael, (2013) A wider role for polyamines in biofilm formation. *Biotechnol Lett* **35**: 1715-1717.

Katoh, K. & D.M. Standley, (2013) MAFFT multiple sequence alignment software version 7: improvements in performance and usability. *Mol Biol Evol* **30**: 772-780.

Kikuchi, Y., O. Kurahashi, T. Nagano & Y. Kamio, (1998) RpoS-dependent expression of the

bioRxiv preprint doi: https://doi.org/10.1101/308080; this version posted May 26, 2018. The copyright holder for this preprint (which was not certified by peer review) is the author/funder. All rights reserved. No reuse allowed without permission.

945 second lysine decarboxylase gene in Escherichia coli. *Biosci Biotechnol Biochem* **62**:
946 1267-1270.
947 Kim, J.S., S.H. Choi & J.K. Lee, (2006) Lysine decarboxylase expression by Vibrio vulnificus is
948 induced by SoxR in response to superoxide stress. *J Bacteriol* **188**: 8586-8592.
949 Kim, S.H., Y. Wang, M. Khomutov, A. Khomutov, C. Fuqua & A.J. Michael, (2016) The
950 Essential Role of Spermidine in Growth of Agrobacterium tumefaciens Is Determined by
951 the 1,3-Diaminopropane Moiety. *ACS Chem Biol* **11**: 491-499.
952 Kuper, C. & K. Jung, (2005) CadC-mediated activation of the cadBA promoter in Escherichia
953 coli. *J Mol Microbiol Biotechnol* **10**: 26-39.
954 Kwon, D.H. & C.D. Lu, (2006) Polyamines induce resistance to cationic peptide,
955 aminoglycoside, and quinolone antibiotics in Pseudomonas aeruginosa PAO1. *Antimicrob*
956 *Agents Chemother* **50**: 1615-1622.
957 Lee, J., A.J. Michael, D. Martynowski, E.J. Goldsmith & M.A. Phillips, (2007) Phylogenetic
958 diversity and the structural basis of substrate specificity in the beta/alpha-barrel fold basic
959 amino acid decarboxylases. *J Biol Chem* **282**: 27115-27125.
960 Lee, Y.S. & Y.D. Cho, (2001) Identification of essential active-site residues in ornithine
961 decarboxylase of Nicotiana glutinosa decarboxylating both L-ornithine and L-lysine.
962 *Biochem J* **360**: 657-665.
963 Letunic, I. & P. Bork, (2016) Interactive tree of life (iTOL) v3: an online tool for the display and
964 annotation of phylogenetic and other trees. *Nucleic Acids Res* **44**: W242-245.
965 Liao, S., P. Poonpairoj, K.C. Ko, Y. Takatuska, Y. Yamaguchi, N. Abe, J. Kaneko & Y. Kamio,
966 (2008) Occurrence of agmatine pathway for putrescine synthesis in Selenomonas
967 ruminatium. *Biosci Biotechnol Biochem* **72**: 445-455.
968 Lightfoot, H.L. & J. Hall, (2014) Endogenous polyamine function--the RNA perspective. *Nucleic*
969 *Acids Res* **42**: 11275-11290.
970 Lohinai, Z., B. Keremi, E. Szoko, T. Tabi, C. Szabo, Z. Tulassay, J.C. DiCesare, C.A. Davis,
971 L.M. Collins & M. Levine, (2015) Biofilm Lysine Decarboxylase, a New Therapeutic
972 Target for Periodontal Inflammation. *J Periodontol* **86**: 1176-1184.
973 Lu, C.D., Z. Yang & W. Li, (2004) Transcriptome analysis of the ArgR regulon in Pseudomonas
974 aeruginosa. *J Bacteriol* **186**: 3855-3861.
975 Madhuri Indurthi, S., H.T. Chou & C.D. Lu, (2016) Molecular characterization of lysR-lysXE,
976 gcdR-gcdHG and amaR-amaAB operons for lysine export and catabolism: a
977 comprehensive lysine catabolic network in Pseudomonas aeruginosa PAO1. *Microbiology*
978 **162**: 876-888.
979 Malet, H., K. Liu, M. El Bakkouri, S.W. Chan, G. Effantin, M. Bacia, W.A. Houry & I. Gutsche,
980 (2014) Assembly principles of a unique cage formed by hexameric and decameric E. coli
981 proteins. *Elife* **3**: e03653.
982 Manuel, J., G.G. Zhanel & T. de Kievit, (2010) Cadaverine suppresses persistence to
983 carboxypenicillins in Pseudomonas aeruginosa PAO1. *Antimicrob Agents Chemother* **54**:
984 5173-5179.
985 McClure MA, S.C., Elton P., (1996) Parameterization studies for the SAM and HMMER
986 methods of hidden markov model generation. In: Proceedings / International Conference
987 on Intelligent Systems for Molecular Biology. pp.
988 Merrell, D.S. & A. Camilli, (2000) Regulation of vibrio cholerae genes required for acid
989 tolerance by a member of the "ToxR-like" family of transcriptional regulators. *J Bacteriol*
990 **182**: 5342-5350.
991 Michael, A.J., (2016a) Biosynthesis of polyamines and polyamine-containing molecules.

bioRxiv preprint doi: https://doi.org/10.1101/308080; this version posted May 26, 2018. The copyright holder for this preprint (which was not certified by peer review) is the author/funder. All rights reserved. No reuse allowed without permission.

Biochem J **473**: 2315-2329.

Michael, A.J., (2016b) Polyamines in Eukaryotes, Bacteria, and Archaea. *J Biol Chem* **291**: 14896-14903.

Miller, J., (1972) Experiments in Molecular Genetics. In. C.S.H.L. Press (ed). Cold Spring Harbor, pp.

Nguyen, L.T., H.A. Schmidt, A. von Haeseler & B.Q. Minh, (2015) IQ-TREE: a fast and effective stochastic algorithm for estimating maximum-likelihood phylogenies. *Mol Biol Evol* **32**: 268-274.

Ochsner, U.A., M.L. Vasil, E. Alsabbagh, K. Parvatiyar & D.J. Hassett, (2000) Role of the Pseudomonas aeruginosa oxyR-recG operon in oxidative stress defense and DNA repair: OxyR-dependent regulation of katB-ankB, ahpB, and ahpC-ahpF. *J Bacteriol* **182**: 4533-4544.

Pezzulo, A.A., X.X. Tang, M.J. Hoegger, M.H. Abou Alaiwa, S. Ramachandran, T.O. Moninger, P.H. Karp, C.L. Wohlford-Lenane, H.P. Haagsman, M. van Eijk, B. Banfi, A.R. Horswill, D.A. Stoltz, P.B. McCray, Jr., M.J. Welsh & J. Zabner, (2012) Reduced airway surface pH impairs bacterial killing in the porcine cystic fibrosis lung. *Nature* **487**: 109-113.

Rahman, M. & P.H. Clarke, (1980) Genes and enzymes of lysine catabolism in Pseudomonas aeruginosa. *J Gen Microbiol* **116**: 357-369.

Ramulu, H.G., M. Groussin, E. Talla, R. Planel, V. Daubin & C. Brochier-Armanet, (2014) Ribosomal proteins: toward a next generation standard for prokaryotic systematics? *Mol Phylogenet Evol* **75**: 103-117.

Romano, A., V. Ladero, M.A. Alvarez & P.M. Lucas, (2014) Putrescine production via the ornithine decarboxylation pathway improves the acid stress survival of Lactobacillus brevis and is part of a horizontally transferred acid resistance locus. *Int J Food Microbiol* **175**: 14-19.

Romano, A., H. Trip, J.S. Lolkema & P.M. Lucas, (2013) Three-component lysine/ornithine decarboxylation system in Lactobacillus saerimneri 30a. *J Bacteriol* **195**: 1249-1254.

Ronquist, F. & J.P. Huelsenbeck, (2003) MrBayes 3: Bayesian phylogenetic inference under mixed models. *Bioinformatics* **19**: 1572-1574.

Schuster, M., A.C. Hawkins, C.S. Harwood & E.P. Greenberg, (2004) The Pseudomonas aeruginosa RpoS regulon and its relationship to quorum sensing. *Mol Microbiol* **51**: 973-985.

Sekowska, A., P. Bertin & A. Danchin, (1998) Characterization of polyamine synthesis pathway in Bacillus subtilis 168. *Mol Microbiol* **29**: 851-858.

Seo, H. & K.J. Kim, (2017) Structural basis for a novel type of cytokinin-activating protein. *Sci Rep* **7**: 45985.

Sevin, D.C., T. Fuhrer, N. Zamboni & U. Sauer, (2017) Nontargeted in vitro metabolomics for high-throughput identification of novel enzymes in Escherichia coli. *Nat Methods* **14**: 187-194.

Shah, P. & E. Swiatlo, (2008) A multifaceted role for polyamines in bacterial pathogens. *Mol Microbiol* **68**: 4-16.

Shan, Y., A. Brown Gandt, S.E. Rowe, J.P. Deisinger, B.P. Conlon & K. Lewis, (2017) ATP-Dependent Persister Formation in Escherichia coli. *MBio* **8**.

Snider, J., I. Gutsche, M. Lin, S. Baby, B. Cox, G. Butland, J. Greenblatt, A. Emili & W.A. Houry, (2006) Formation of a distinctive complex between the inducible bacterial lysine decarboxylase and a novel AAA+ ATPase. *J Biol Chem* **281**: 1532-1546.

Soksawatmaekhin, W., A. Kuraishi, K. Sakata, K. Kashiwagi & K. Igarashi, (2004) Excretion

bioRxiv preprint doi: https://doi.org/10.1101/308080; this version posted May 26, 2018. The copyright holder for this preprint (which was not certified by peer review) is the author/funder. All rights reserved. No reuse allowed without permission.

and uptake of cadaverine by CadB and its physiological functions in Escherichia coli. *Mol Microbiol* **51**: 1401-1412.

Stover, C.K., X.Q. Pham, A.L. Erwin, S.D. Mizoguchi, P. Warrener, M.J. Hickey, F.S. Brinkman, W.O. Hufnagle, D.J. Kowalik, M. Lagrou, R.L. Garber, L. Goltry, E. Tolentino, S. Westbrock-Wadman, Y. Yuan, L.L. Brody, S.N. Coulter, K.R. Folger, A. Kas, K. Larbig, R. Lim, K. Smith, D. Spencer, G.K. Wong, Z. Wu, I.T. Paulsen, J. Reizer, M.H. Saier, R.E. Hancock, S. Lory & M.V. Olson, (2000) Complete genome sequence of Pseudomonas aeruginosa PAO1, an opportunistic pathogen. *Nature* **406**: 959-964.

Sugawara, A., D. Matsui, N. Takahashi, M. Yamada, Y. Asano & K. Isobe, (2014) Characterization of a pyridoxal-5'-phosphate-dependent l-lysine decarboxylase/oxidase from Burkholderia sp. AIU 395. *J Biosci Bioeng* **118**: 496-501.

Tabor, C.W. & H. Tabor, (1985) Polyamines in microorganisms. *Microbiol Rev* **49**: 81-99.

Tabor, H., E.W. Hafner & C.W. Tabor, (1980) Construction of an Escherichia coli strain unable to synthesize putrescine, spermidine, or cadaverine: characterization of two genes controlling lysine decarboxylase. *J Bacteriol* **144**: 952-956.

Tabor, H. & C.W. Tabor, (1964) Spermidine, Spermine, and Related Amines. *Pharmacol Rev* **16**: 245-300.

Takatsuka, Y., Y. Yamaguchi, M. Ono & Y. Kamio, (2000) Gene cloning and molecular characterization of lysine decarboxylase from Selenomonas ruminantium delineate its evolutionary relationship to ornithine decarboxylases from eukaryotes. *J Bacteriol* **182**: 6732-6741.

Thibault, J., E. Faudry, C. Ebel, I. Attree & S. Elsen, (2009) Anti-activator ExsD forms a 1:1 complex with ExsA to inhibit transcription of type III secretion operons. *J Biol Chem* **284**: 15762-15770.

Valot, B., C. Guyeux, J.Y. Rolland, K. Mazouzi, X. Bertrand & D. Hocquet, (2015) What It Takes to Be a Pseudomonas aeruginosa? The Core Genome of the Opportunistic Pathogen Updated. *PLoS One* **10**: e0126468.

Viala, J.P., S. Meresse, B. Pocachard, A.A. Guilhon, L. Aussel & F. Barras, (2011) Sensing and adaptation to low pH mediated by inducible amino acid decarboxylases in Salmonella. *PLoS One* **6**: e22397.

Zhao, B. & W.A. Houry, (2010) Acid stress response in enteropathogenic gammaproteobacteria: an aptitude for survival. *Biochem Cell Biol* **88**: 301-314.

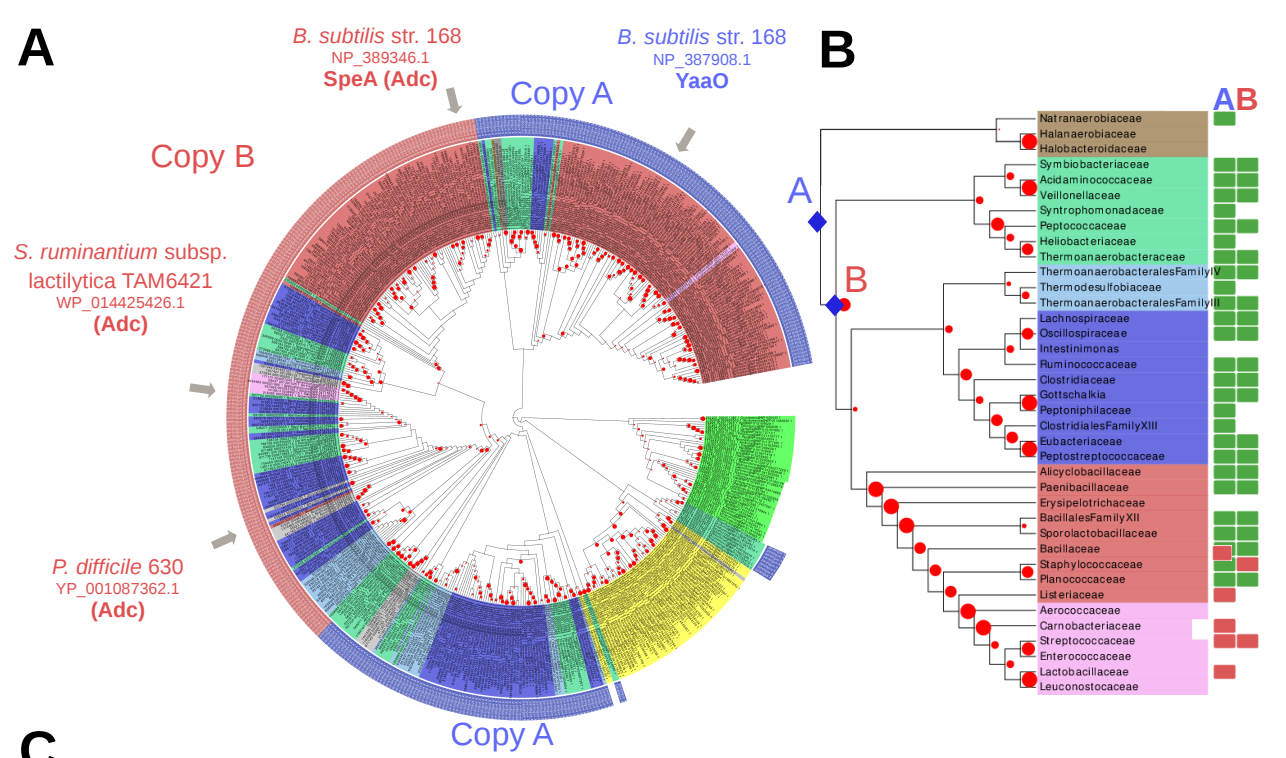

C

A

Peptoclostridium difficile 630
YP_001090072.1
NC_009089.1 (genomic)

Selenomonas ruminantium subsp. lactilytica TAM6421
WP_014423651.1
NC_017068.1 (chromosome)

Bacillus subtilis subsp. subtilis str. 168
NP_387908.1
NC_000964.3 (chromosome)

Paenibacillus bovis BD3526
WP_060531710.1
NZ_CP013023.1 (chromosome)

B

Peptoclostridium difficile 630
YP_001087362.1
NC_009089.1 (genomic)

Selenomonas ruminantium subsp. lactilytica TAM6421
WP_014425426.1
NC_017068.1 (chromosome)

Bacillus subtilis subsp. subtilis str. 168
NP_389346.1
NC_000964.3 (chromosome)

Paenibacillus bovis BD3526
WP_060535746.1
NZ_CP013023.1 (chromosome)

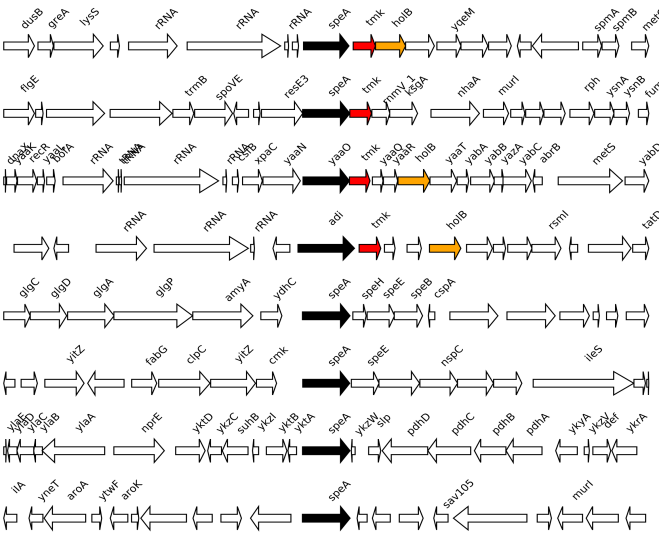

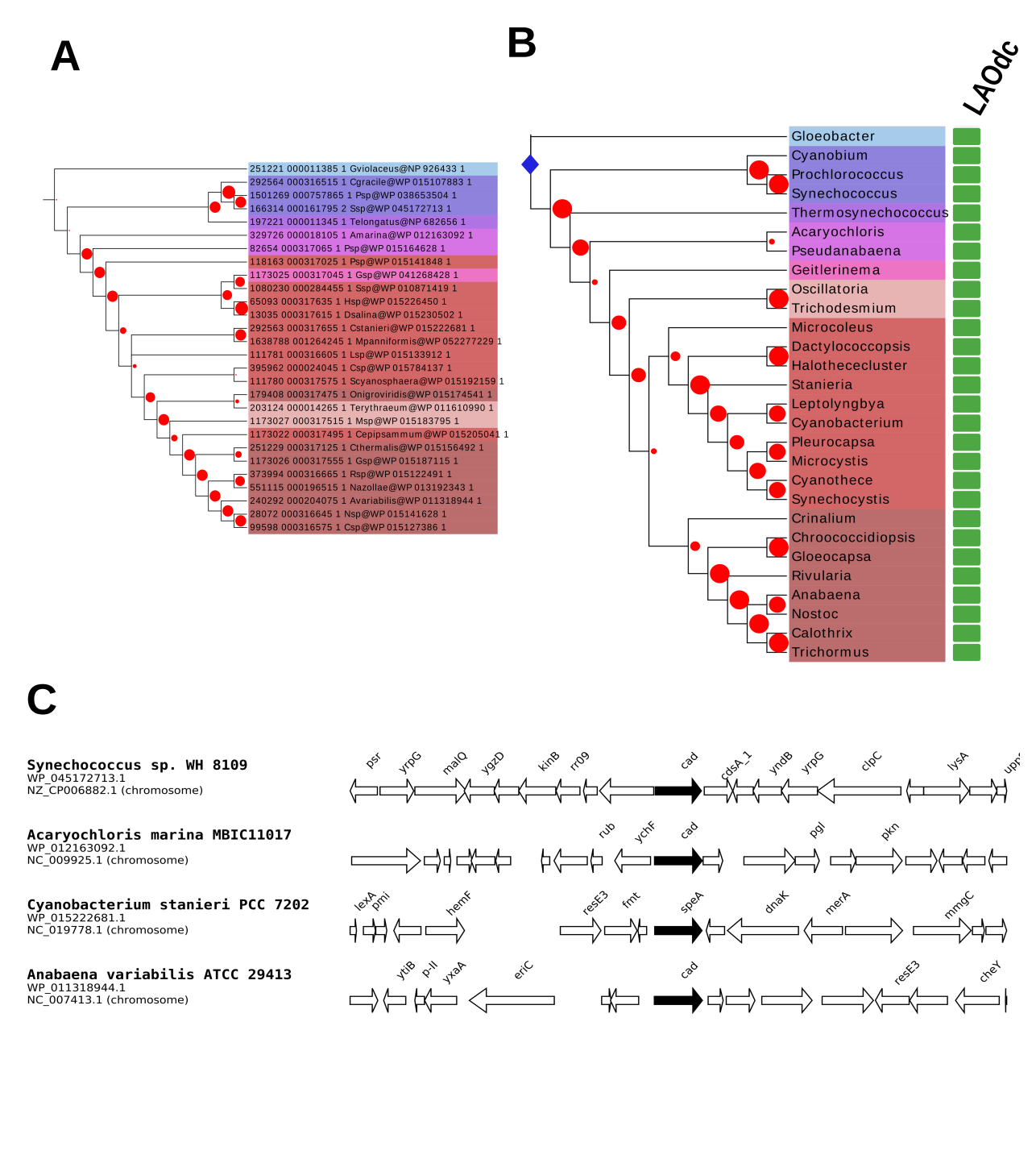
A
251221 000011385 1 Gviolaceus@NP 926433 1
292564 000316515 1 Cgracile@WP 015107883 1
1501269 000757865 1 Psp@WP 038653504 1
166314 000161795 2 Ssp@WP 045172713 1
197221 000011345 1 Telongatus@NP 682656 1
329726 000018105 1 Amarina@WP 012163092 1
82654 000317065 1 Psp@WP 015164628 1
118163 000317025 1 Psp@WP 015141848 1
1173025 000317045 1 Gsp@WP 041268428 1
1080230 000284455 1 Ssp@WP 010871419 1
65093 000317635 1 Hsp@WP 015226450 1
13035 000317615 1 Dsalina@WP 015230502 1
292563 000317655 1 Cstanieri@WP 015222681 1
1638788 001264245 1 Mpanniformis@WP 052277229 1
111781 000316605 1 Lsp@WP 015133912 1
395962 000024045 1 Csp@WP 015784137 1
111780 000317575 1 Scyanosphaera@WP 015192159 1
179408 000317475 1 Onigroviridis@WP 015174541 1
203124 000014265 1 Terythraeum@WP 011610990 1
1173027 000317515 1 Msp@WP 015183795 1
1173022 000317495 1 Cepipsammum@WP 015205041 1
251229 000317125 1 Cthermalis@WP 015156492 1
1173026 000317555 1 Gsp@WP 015187115 1
373994 000316665 1 Rsp@WP 015122491 1
551115 000196515 1 Nazollae@WP 013192343 1
240292 000204075 1 Avariabilis@WP 011318944 1
28072 000316645 1 Nsp@WP 015141628 1
99598 000316575 1 Csp@WP 015127386 1
B
LAOdc
Gloeobacter
Cyanobium
Prochlorococcus
Synechococcus
Thermosynechococcus
Acaryochloris
Pseudanabaena
Geitlerinema
Oscillatoria
Trichodesmium
Microcoleus
Dactylococcopsis
Halothececluster
Stanieria
Leptolyngbya
Cyanobacterium
Pleurocapsa
Microcystis
Cyanothece
Synechocystis
Crinalium
Chroococcidiopsis
Gloeocapsa
Rivularia
Anabaena
Nostoc
Calothrix
Trichormus
C
Synechococcus sp. WH 8109
WP_045172713.1
NZ_CP006882.1 (chromosome)
psr yrpG malQ ygzD kinB rr09 cad cdsA_1 yndB yrpG clpC lysA upp
Acaryochloris marina MBIC11017
WP_012163092.1
NC_009925.1 (chromosome)
rub ychF cad pgl pkn
Cyanobacterium stanieri PCC 7202
WP_015222681.1
NC_019778.1 (chromosome)
lexA pmi hemF resE3 fmt speA dnaK merA mmgC
Anabaena variabilis ATCC 29413
WP_011318944.1
NC_007413.1 (chromosome)
ytiB p-II yxaA eriC cad resE3 cheY

A

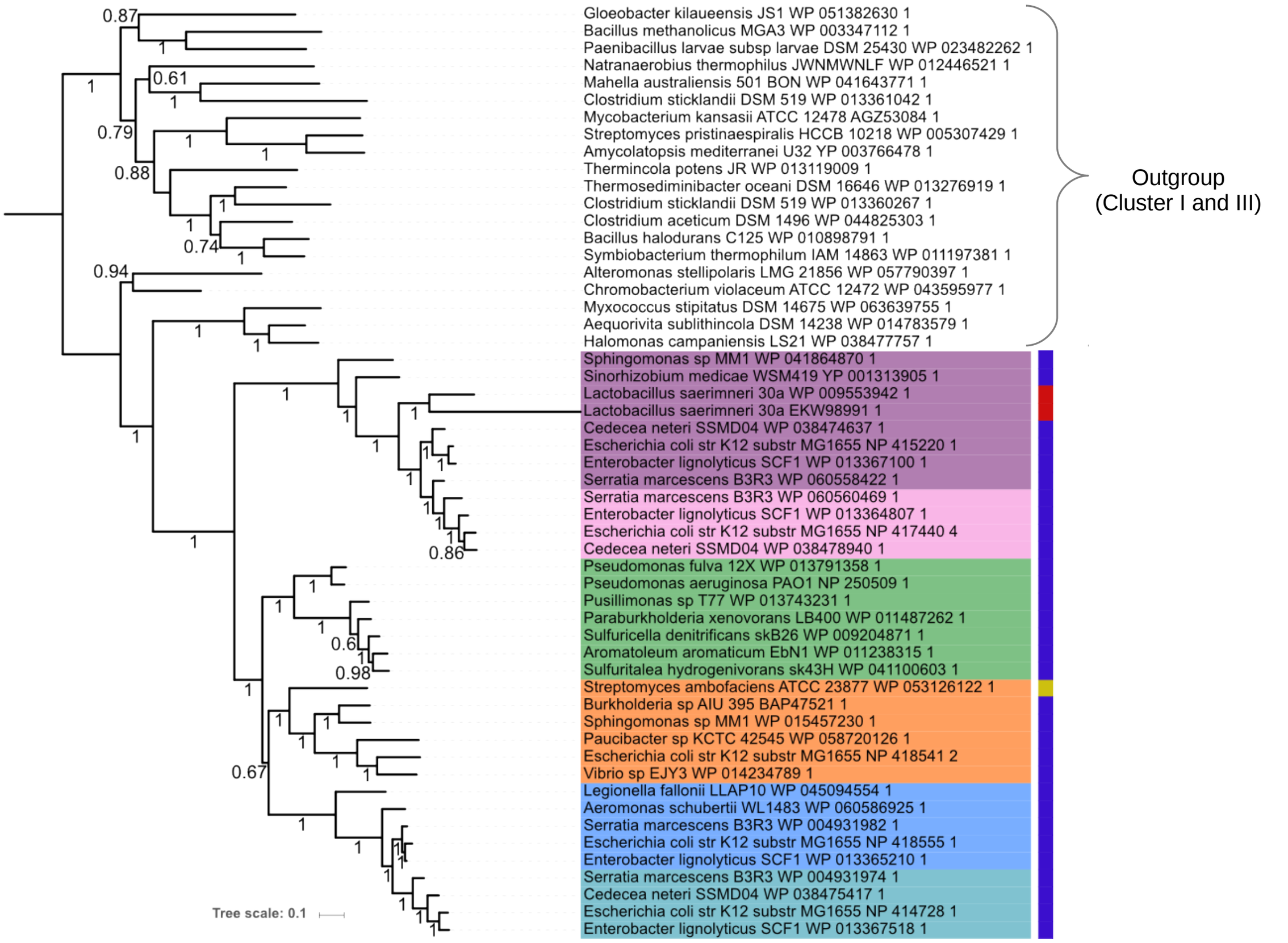

B

bioRxiv preprint doi: https://doi.org/10.1101/308080; this version posted May 26, 2018. The copyright holder for this preprint (which was not certified by peer review) is the author/funder. All rights reserved. No reuse allowed without permission.

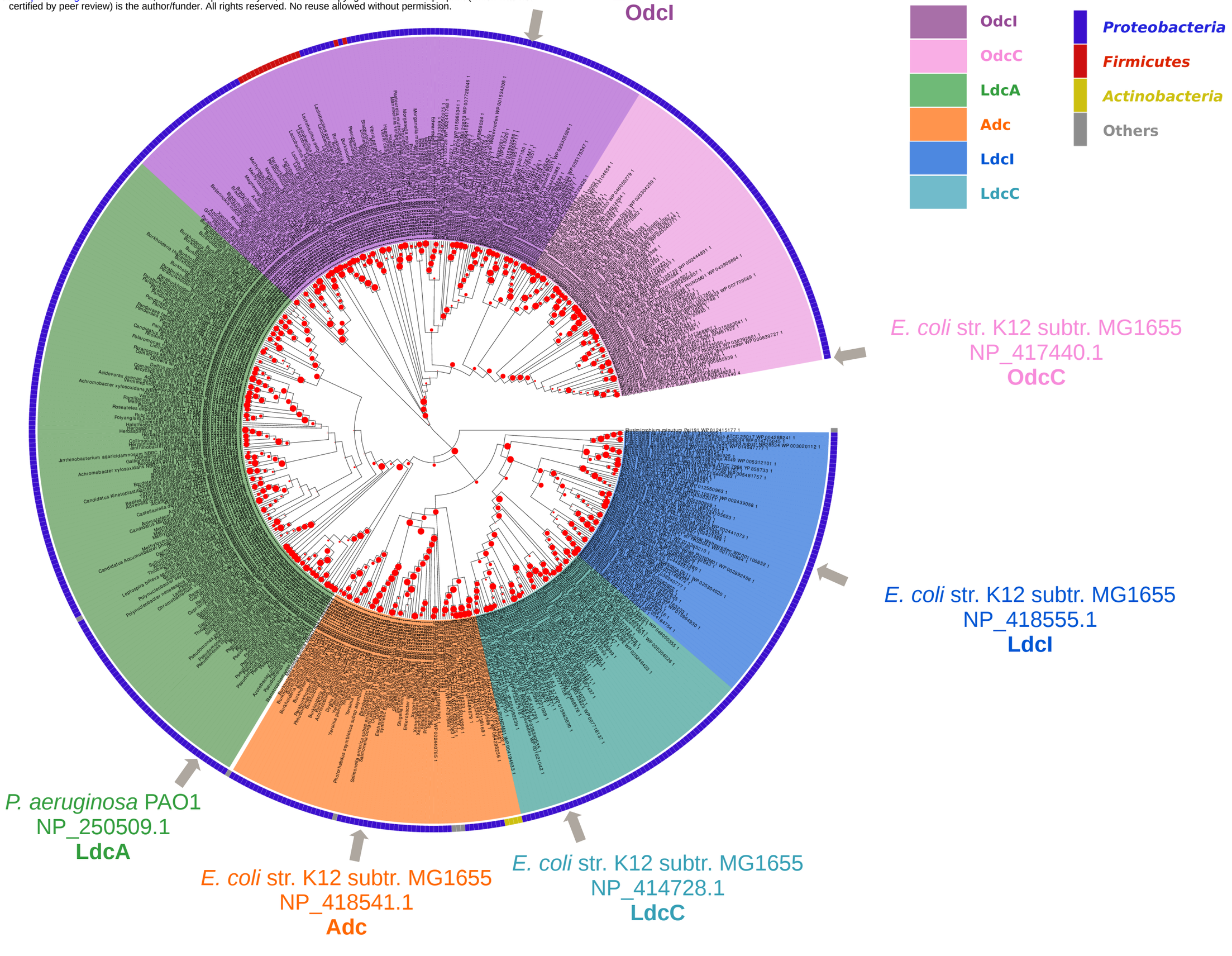

bioRxiv preprint doi: https://doi.org/10.1101/308080; this version posted May 26, 2018. The copyright holder for this preprint (which was not certified by peer review) is the author/funder. All rights reserved. No reuse allowed without permission.

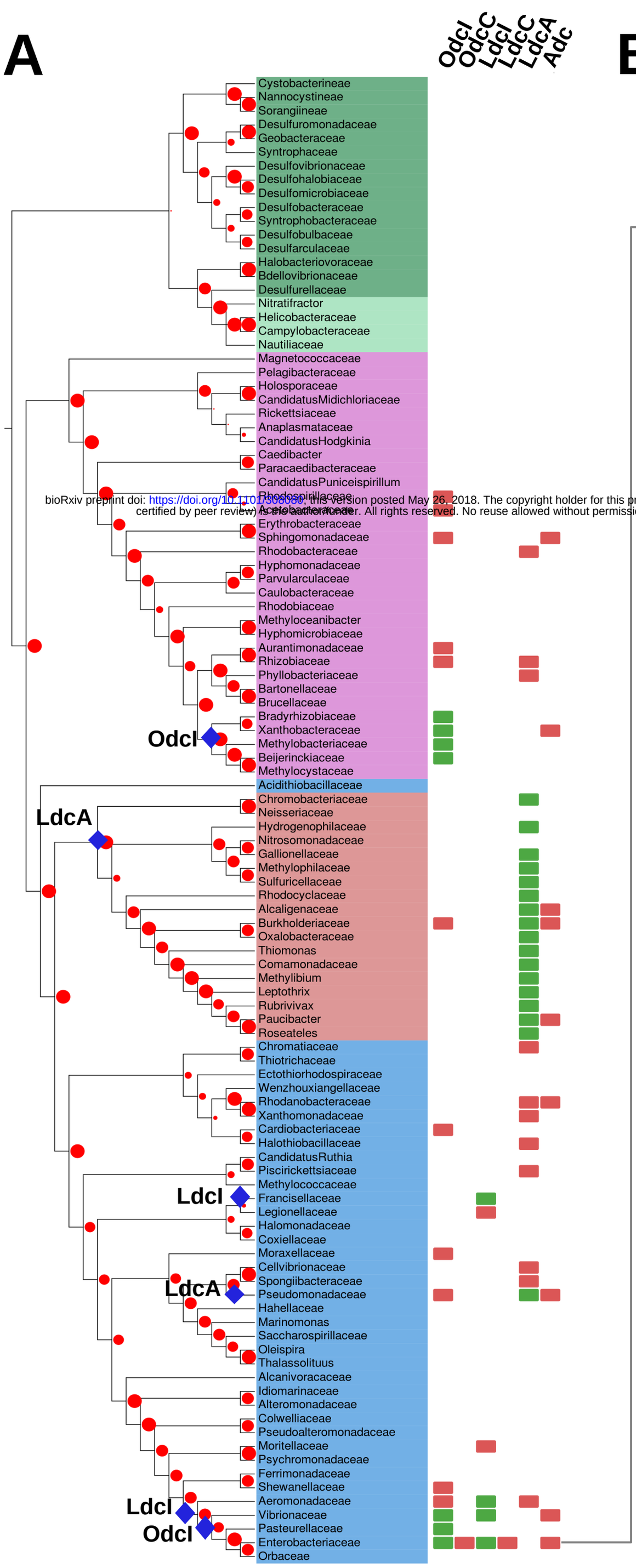

bioRxiv preprint doi: https://doi.org/10.1101/308080; this version posted May 26, 2018. The copyright holder for this preprint (which was not certified by peer review) is the author/funder. All rights reserved. No reuse allowed without permission.

A

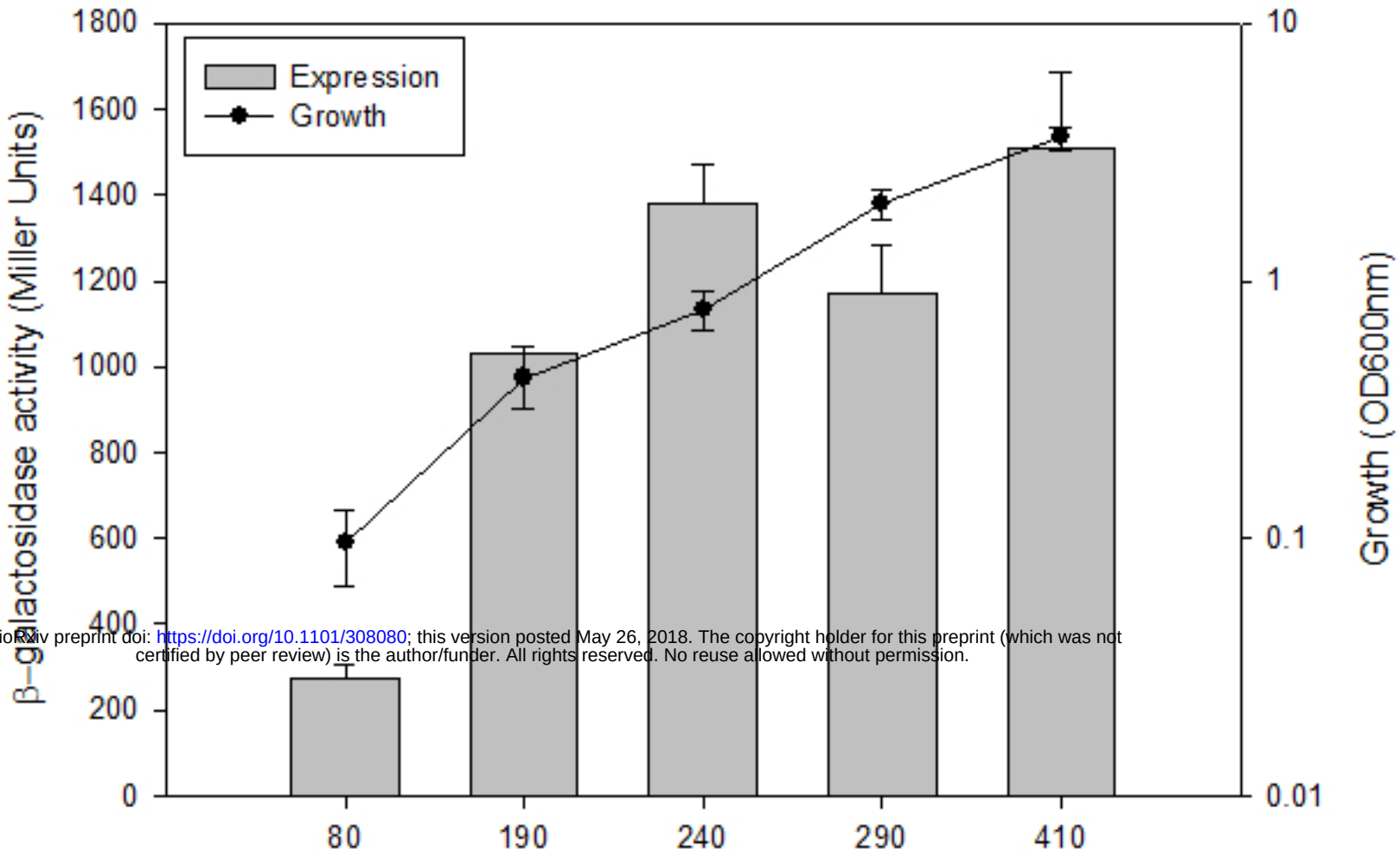

B

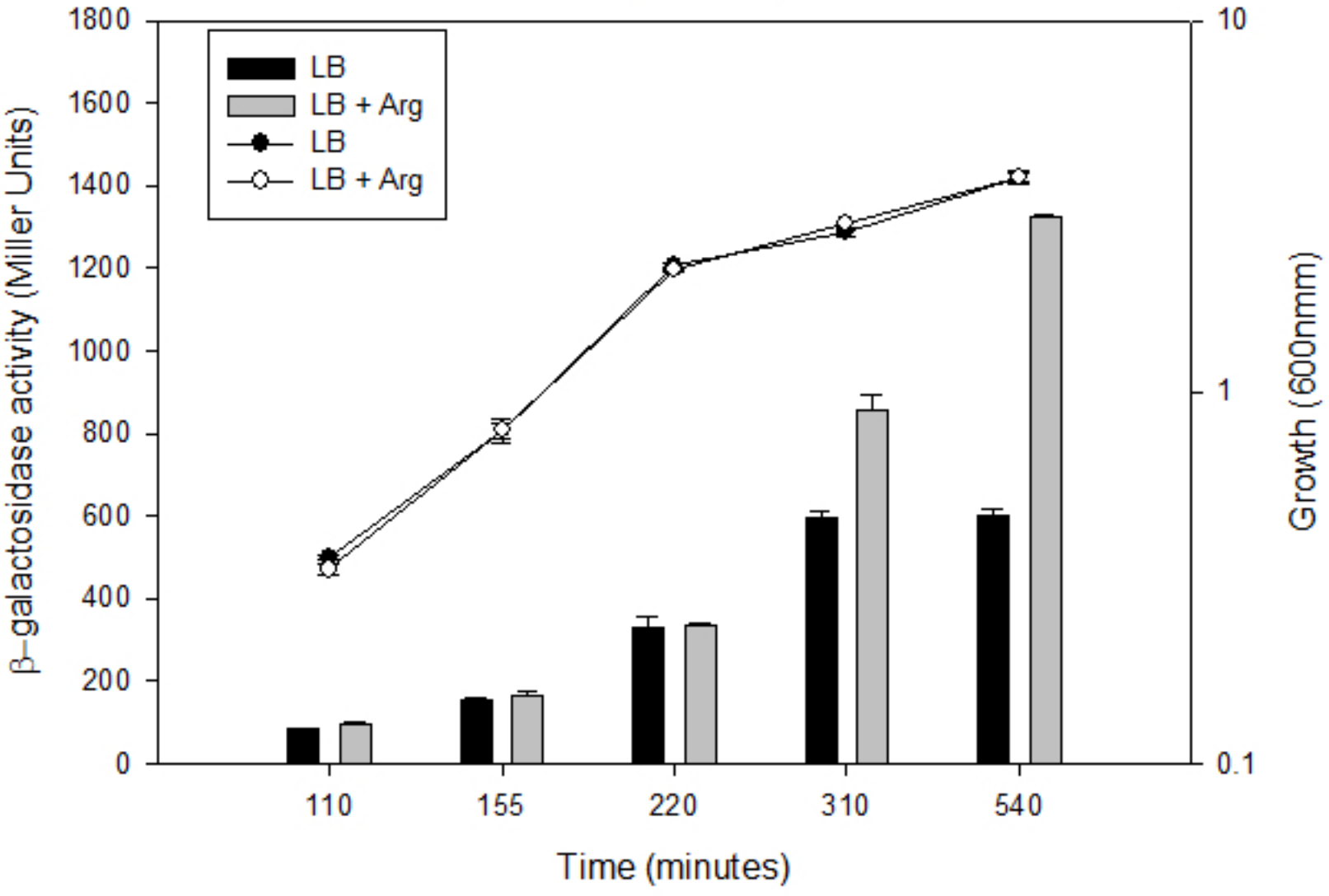

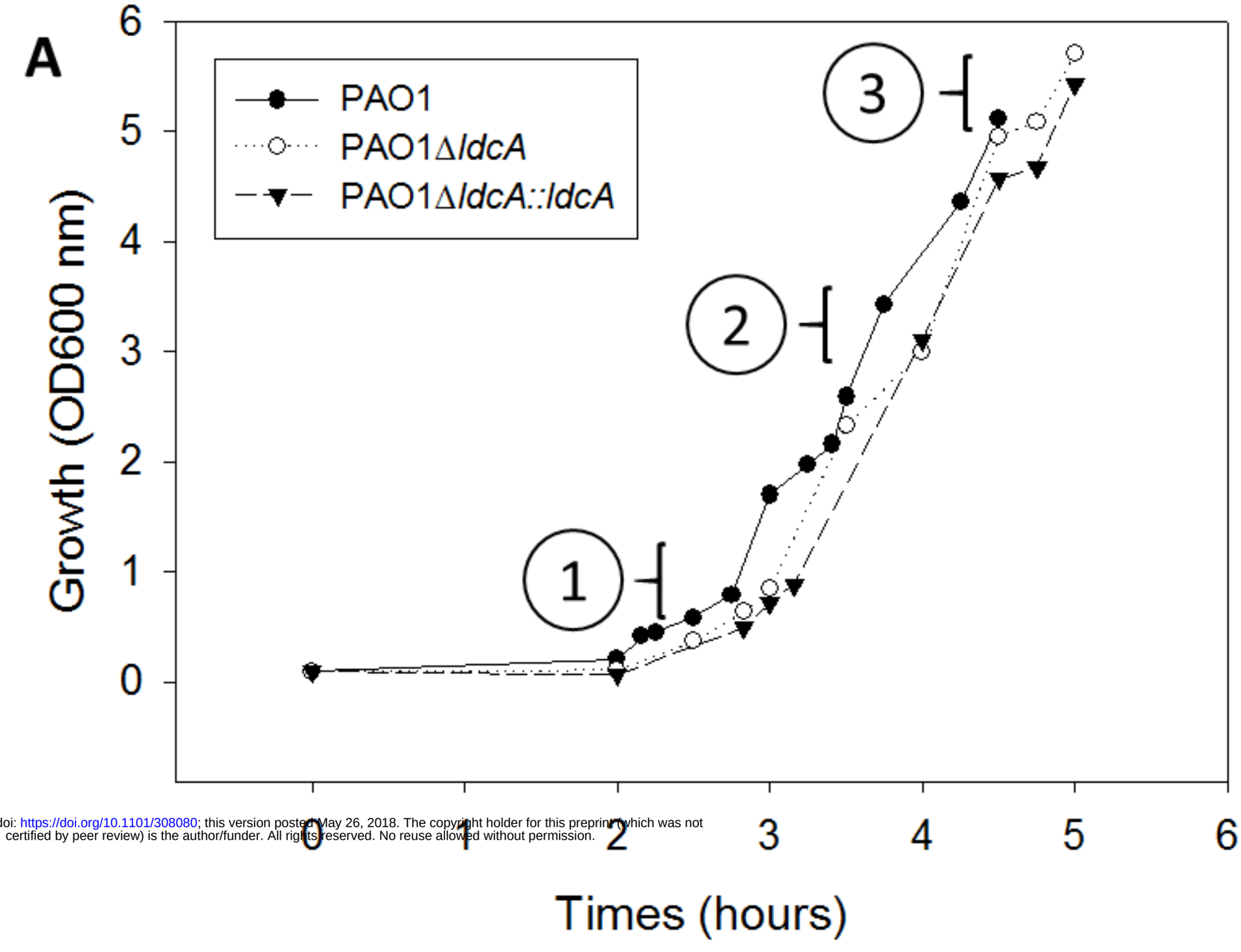

bioRxiv preprint doi: https://doi.org/10.1101/308080; this version posted May 26, 2018. The copyright holder for this preprint (which was not certified by peer review) is the author/funder. All rights reserved. No reuse allowed without permission.

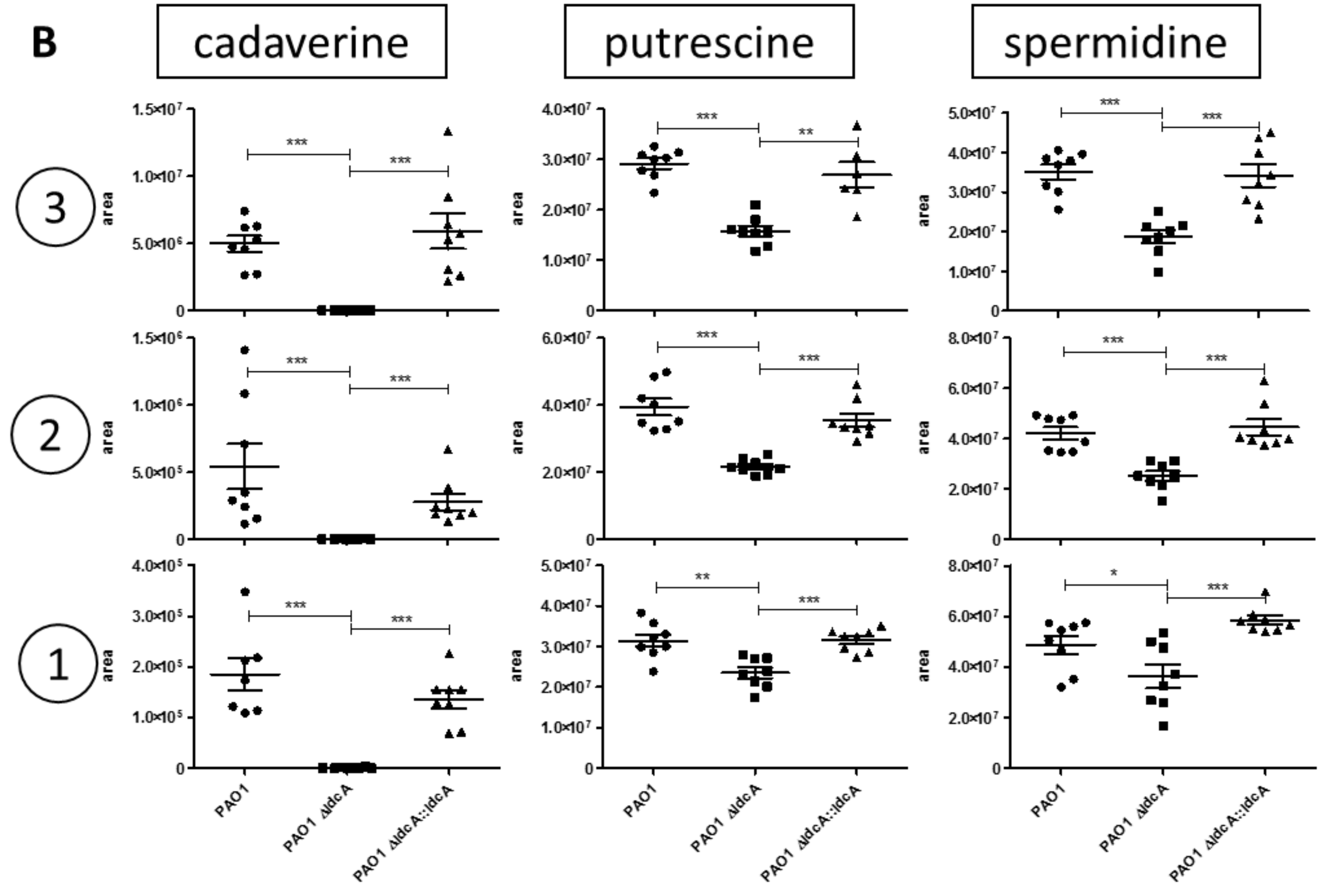

bioRxiv preprint doi: https://doi.org/10.1101/308080; this version posted May 26, 2018. The copyright holder for this preprint (which was not certified by peer review) is the author/funder. All rights reserved. No reuse allowed without permission.